Calhoun: The NPS Institutional Archive

Theses and Dissertations | Thesis Collection

1992

Correlation of processing, microstructure, and superplasticity in an Al-MG-ZR alloy.

Lyle, Peter C.

Monterey, California. Naval Postgraduate School

http://hdl.handle.net/10945/23595

http://www.nps.edu/library

Calhoun is a project of the Dudley Knox Library at NPS, furthering the precepts and goals of open government and government transparency. All information contained herein has been approved for release by the NPS Public Affairs Officer.

Dudley Knox Library / Naval Postgraduate School
411 Dyer Road / 1 University Circle
Monterey, California USA 93943

DUDLEY KNOX LIBRARY
NAVAL POSTGRADUATE SCHOOL
MONTEREY CA 93943-5101

Approved for public release; distribution is unlimited.

CORRELATION OF PROCESSING, MICROSTRUCTURE, AND SUPERPLASTICITY IN AN Al-MG-ZR ALLOY

by

PETER C. LYLE
Lieutenant, United States Navy
B.S.M.E., Massachusetts Maritime Academy, 1986

Submitted in partial fulfillment of the
requirements for the degree of

MASTER OF SCIENCE IN MECHANICAL ENGINEERING

from the

NAVAL POSTGRADUATE SCHOOL
March 20, 1992

Anthony J. Healy, Chairman
Department of Mechanical Engineering

REPORT DOCUMENTATION PAGE

Form Approved
OMB No. 0704-0188

a REPORT SECURITY CLASSIFICATION UNCLASSIFIED	1b RESTRICTIVE MARKINGS
a SECURITY CLASSIFICATION AUTHORITY	3 DISTRIBUTION / AVAILABILITY OF REPORT Approved for public release; distribution is unlimited.
b DECLASSIFICATION / DOWNGRADING SCHEDULE	
PERFORMING ORGANIZATION REPORT NUMBER(S)	5 MONITORING ORGANIZATION REPORT NUMBER(S)
NAME OF PERFORMING ORGANIZATION Naval Postgraduate School 6b OFFICE SYMBOL (If applicable) ME	7a NAME OF MONITORING ORGANIZATION Naval Postgraduate School
ADDRESS (City, State, and ZIP Code) Monterey, CA 93943-5000	7b ADDRESS (City, State, and ZIP Code) Monterey, CA 93943-5000
NAME OF FUNDING / SPONSORING ORGANIZATION 8b OFFICE SYMBOL (If applicable)	9 PROCUREMENT INSTRUMENT IDENTIFICATION NUMBER
ADDRESS (City, State, and ZIP Code)	10 SOURCE OF FUNDING NUMBERS PROGRAM ELEMENT NO / PROJECT NO / TASK NO / WORK UNIT ACCESSION NO

TITLE (Include Security Classification)

CORRELATION OF PROCESSING, MICROSTRUCTURE, AND SUPERPLASTICITY IN AN AL-MG-ZR ALLOY

PERSONAL AUTHOR(S)

Lyle, Peter C.

a TYPE OF REPORT	13b TIME COVERED	14 DATE OF REPORT (Year, Month, Day)	15 PAGE COUNT
Master's Thesis	FROM _____ TO _____	March 1992	74

SUPPLEMENTARY NOTATION The views expressed in this thesis are those of the author and do ot reflect the official policy or position of the Department of Defense or the U.S. Gov't

COSATI CODES		
FIELD	GROUP	SUB-GROUP

18 SUBJECT TERMS (Continue on reverse if necessary and identify by block number)

superplasticity, particle stimulated nucleation, Aluminum-Magnesium alloys

ABSTRACT (Continue on reverse if necessary and identify by block number)

Investigation of the influence of the strain history during thermomechanical processing of an Al-10Mg-0.1Zr was conducted. Refined, recrystallized microstructures resulted when larger strains were employed in the later passes of the TMP. Superplastic responses up to approximately 420 percent were obtained. Conversely, when smaller strains were at the later stages of the TMP, less recrystallized, coarser structures resulted, and the corresponding superplastic ductilities of approximately 280 percent were obtained.

DISTRIBUTION / AVAILABILITY OF ABSTRACT ☒ UNCLASSIFIED/UNLIMITED ☐ SAME AS RPT ☐ DTIC USERS	21 ABSTRACT SECURITY CLASSIFICATION Unclassified
a NAME OF RESPONSIBLE INDIVIDUAL T.R. McNelley	22b TELEPHONE (Include Area Code) (408) 646-2589 22c OFFICE SYMBOL ME/Mc

Form 1473, JUN 86 Previous editions are obsolete. SECURITY CLASSIFICATION OF THIS PAGE

S/N 0102-LF-014-6603

Unclassified

ABSTRACT

Investigation of the influence of the strain history during thermomechanical processing of an Al-10Mg-0.1Zr was conducted. Refined, recrystallized microstructures resulted when larger strains were employed in the later passes of the TMP. Superplastic responses up to approximately 420 percent were obtained. Conversely, when smaller strains were at the later stages of the TMP, less recrystallized, coarser structures resulted, and the corresponding superplastic ductilities of approximately 280 percent were obtained.

TABLE OF CONTENTS

DUDLEY KNOX LIBRARY
NAVAL POSTGRADUATE SCHOOL
MONTEREY CA 93943-5101

LIST OF TABLES

LIST OF FIGURES

ACKNOWLEDGEMENTS

I would like to express my sincere thanks to Professor Terry McNelley and Professor Peter Kalu for their invaluable assistance, guidance, and ever present support throughout the course of my research. I would also like to express my thanks to Professor Roy Crooks, Doug Shelton, and Tom McCord for their technical assistance. Finally, I would like to say thank you to my wife Patty, who has been an ear, shoulder, and spoon during these last two school years.

I. INTRODUCTION

Superplasticity is the term used to describe the ability of a material to undergo large, tensile plastic deformation without localized necking. Elongations greater than 200% are considered superplastic, and elongations greater than 1000% are not uncommon. This phenomenon is extensively used in fabrications involving complex shapes.

The commercial impacts of superplastic forming have included lower production costs and decreased overall production times, while maintaining high dimensional accuracy of lighter weight components. Superplastically formed components can replace otherwise heavier built-up assemblies that require fastening of numerous individual parts. Reduction or elimination of fasteners means lower susceptibility to stress concentrations, fatigue and corrosion as well as reduced weight.

Due to these advantages, superplastic forming is especially attractive to the aerospace community. Current applications of superplastic metals include wing components for the Airbus A300, missile flaps, light weight coolant piping, radar dishes and compass stabilizer units to name only a few [Ref. 1].

By nature, metals and alloys are not superplastic. However, the introduction of additional components to the alloy composition and/or thermomechanical

processing (TMP) may render the material superplastic. The basic requirements for superplastic behavior are fine, recrystallized and equiaxed grains and second phase precipitates that will inhibit grain growth at elevated temperatures.

The earliest utilization of TMP to improve the formability of aluminum was by Anderson in 1918, who improved the formability by controlling the cold rolling and annealing processes [Ref. 2, 3]. In 1976 it was reported by Watts, et al [Ref. 4], that useful superplastic aluminum alloys had been developed and subsequently it has been shown that by careful control of thermal and mechanical processing a broader range of microstructural responses would result.

Current work at the Naval Postgraduate School (NPS) has focused on making several aluminum alloys superplastic at low temperatures (~300°C). Factors of the TMPs found to influence subsequent ductility include: temperature, time at temperature, reheat interval and strain history. The purpose of this research is to examine the effect strain history has upon the superplastic response of an Al-10Mg-0.1Zr alloy.

II. BACKGROUND

In order to obtain a superplastic response, certain microstructural criteria must first be met. Fine equiaxed grains, typically less than 10μm in size, and the presence of uniformly dispersed second phase particles that will inhibit grain growth are considered basic requirements for superplasticity. The two principle factors that will determine if the criteria will be met are alloy composition and the thermomechanical processing to be conducted upon the material.

A. DEVELOPMENT OF THE ALLOY

1. Solid Solution Strengthening

Al-10Mg-0.1Zr may be considered as a 5xxx series, non-heat-treatable aluminum alloy. The solid solubility of Mg in Al is approximately 14.9% at the eutectic temperature of 451°C [Ref. 5], as shown in the phase diagram of Figure 1. Magnesium in solution in aluminum imparts significant hardening effect [Ref. 2].

2. Precipitation

Precipitation of second phase from a supersaturated solid solution does not provide a direct strengthening mechanism in the Al-Mg alloy. The precipitation reaction is represented in equation 1 [Ref. 6]:

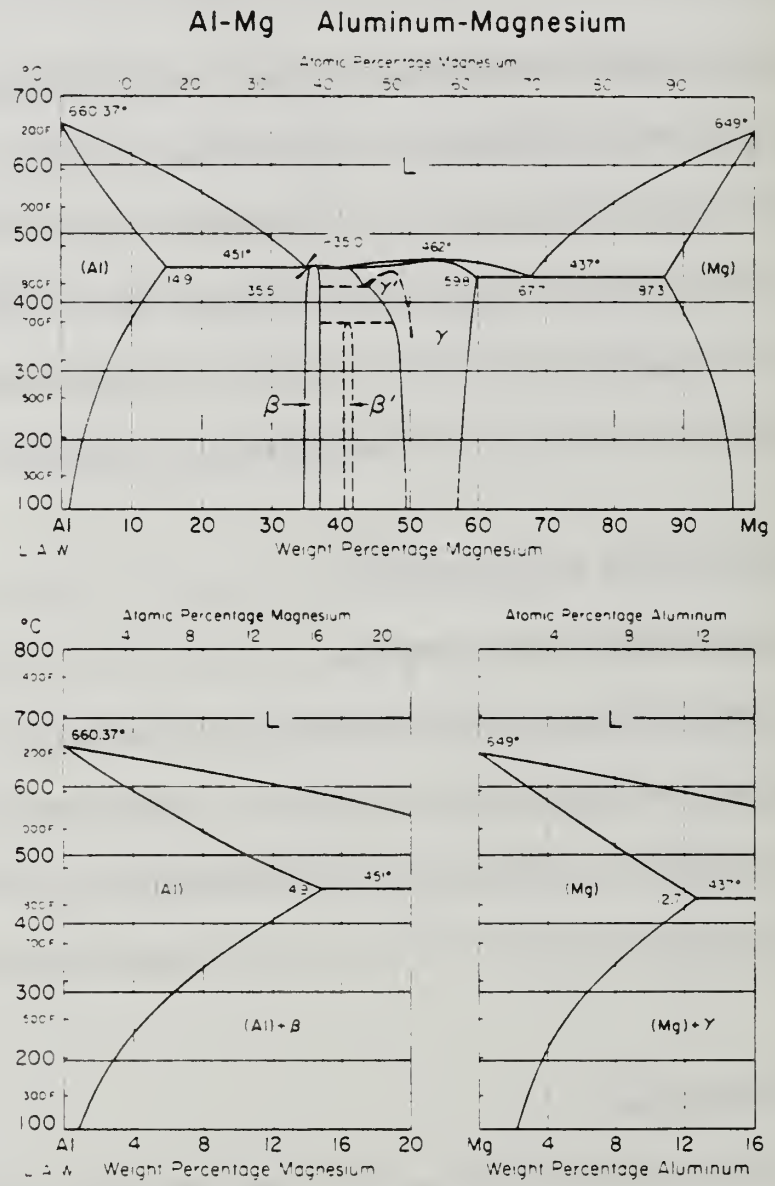

Figure 1. Phase Diagram of Al-Mg Alloy System.

Supersaturated Solution → $Al+\beta(Mg_5Al)$ **Equation 1**

The β precipitate is not a coherent precipitate in the matrix, but rather an incoherent phase which forms initially along prior grain boundaries. The β phase, although not a strengthening agent, when uniformly distributed within the matrix and of sufficient size and quantity, is critical in the recrystallization during processing of the material. This second-phase precipitate may also inhibit grain growth when the material is subjected to required elevated superplastic temperatures [Ref 6]. Recent studies have shown that the β phase particles in the matrix can increase in size beyond the critical size necessary to stimulate particle stimulated nucleation of recrystallization. One of the objectives of this thesis is to understand under what conditions this mechanism occurs in Al-Mg alloys.

3. Dispersion Strengthening

The addition of Zirconium (Zr) to the Al-Mg alloy may result in an additional precipitation of second phase particle ($ZrAl_3$). These second phase particles, called dispersoids, are insoluble at high temperatures and are much harder than the surrounding matrix [Ref. 7]. The Zr content here is not sufficient to provide large amounts of $ZrAl_3$. Most of the Zr remains in solution and the exact role of zirconium is not clearly understood. Dispersoids of $ZrAl_3$ aid in controlling the recrystallization of fine grain structures, which is needed for superplasticity, but the role of Zr in solid solution has not been clearly identified.

B. DEVELOPMENT OF THE THERMOMECHANICAL PROCESS (TMP)

During thermomechanical processing, deformation bands form, grains change shape, second-phase particles precipitate, and substructure develops due to recovery. At some point, recrystallization may also take place. The controlling factors of the aforementioned are temperature, time at temperature and strain history. The goal of the TMP here is to manipulate the controlling factors to produce a refined structure, stabilized by second phase particles so that when tensile deformation is performed the material will respond superplastically.

Warm rolling follows an initial solid solution treatment and hot forging of the billets. The term "warm" is used because rolling is performed at a temperature below the β-phase solvus temperature. During rolling, dislocations are generated and become pinned at sites of obstructions such as previous grain boundaries, dispersoids and precipitates. The generation rate of dislocations is dependent on the strain rate [Ref. 2], and increasing strain rates on successive passes has been employed in TMP schedules.

Previous work at NPS has utilized sequential warm rolling passes and static anneals below the solvus. Table I is the rolling schedule developed by Gorsuch [Ref. 8]. That research investigated the effect of the reheating duration between passes (time at temperature). Gorsuch reported ductilities greater than 1100% when a 30-minute reheating interval between each pass was employed. It was also demonstrated [Ref. 9] that increasing the reheating interval

between passes had marked improvement of superplastic ductility of an Al-10Mg-0.1Zr alloy.

TABLE I. GORSUCH ROLLING SCHEDULE

PASS	hi (in)	Δh (in)	ε (%)	$\dot{\varepsilon}$ (S^{-1})
1	0.94	0.10	10.6	0.95
2	0.84	0.10	11.9	1.07
3	0.74	0.10	13.5	1.22
3	0.64	0.10	15.6	1.41
5	0.54	0.10	18.5	1.69
6	0.44	0.10	22.7	2.09
7	0.34	0.10	29.4	2.75
8	0.24	0.06	25.0	2.99
9	0.18	0.05	27.8	3.66
10	0.14	0.04	30.8	4.57
11	0.09	0.03	33.3	5.74
12	0.06	0.013	21.7	5.52

In this research, an attempt to duplicate Gorsuch's rolling schedule was made. Furthermore, modified versions incorporating larger reductions (strains) in the later passes of the TMP are conducted. These alterations were designed to produce equal or finer grain structures.

In Gorsuch's rolling schedule the sample thickness after each pass was not measured and so the values of strain and strain rate do not reflect mill deflection

[Ref. 10]. Thus, equations 2 and 3 were used to modify Gorsuch's rolling schedule. Equation 4 was utilized to calculate accumulated strain.

$$\epsilon = \frac{h_i - h_f}{h_i} \times 100 = \frac{\Delta h}{h_i} \times 100 \qquad \text{Equation 2}$$

$$\dot{\epsilon} = \frac{2\pi Rn}{\sqrt{Rh_i}} \sqrt{\epsilon}\left(1 + \frac{\epsilon_p}{4}\right) \qquad \text{Equation 3}$$

$$\epsilon = -Ln\left(1 - \frac{h_o - h_c}{h_o}\right) \qquad \text{Equation 4}$$

where ε is the strain associated with the rolling pass; $\dot{\varepsilon}$ is the strain rate; h_o thickness prior to rolling; h_i thickness prior to individual passes; h_f thickness after individual passes; Δh is the material's thickness reduction; h_c thickness at the conclusion of processing; R is radius of the rollers; n is the speed of the rollers (rads/s).

C. MICROSTRUCTURAL DEVELOPMENT AND PSN

The evolution of an Al-Mg-Zr alloy structure during thermomechanical processing has been discussed [Ref. 11]. The microstructural evolution of similar alloys processed at NPS has also been presented [Ref. 10].

When materials containing large, hard, second-phase particles, in a deformable matrix are deformed, dislocation densities in association with deformation zones may be formed in the vicinity of the particles. These zones consist of highly misoriented grains or subgrains and are usually developed at particles greater than 1.0 μm in size [Ref. 12]. If the material is subsequently annealed at elevated temperatures, recrystallization may be initiated at these particles leading to particle stimulated nucleation (PSN) of recrystallization.

In this research, the effect of larger strains on the development of deformation zones at second-phase particles and subsequent recrystallization will be investigated. It is believed that larger strains will create more intense deformation zones at larger particles that will promote particle stimulated nucleation of finer grain structures.

D. MECHANISMS OF SUPERPLASTIC FLOW

Superplastic alloys exhibit resistance to localized necking during deformation at elevated temperatures (0.5 - 0.65T_m). The resistance to localized necking is dependent on the material's strain rate sensitivity coefficient. Flow stress can be related to the strain rate as follows:

$$\sigma = K\dot{\varepsilon}^m \qquad \textbf{Equation 5}$$

where σ is the flow stress, $\dot{\varepsilon}$ is the strain rate, K is a material constant and m is also a material constant termed the strain rate sensitivity coefficient [Ref. 13]. As the value of m increases, the flow stress and thus resistance to localized plastic flow (necking) increases and consequently elongation to failure increases. When the relationship between σ and $\dot{\varepsilon}$ becomes linear (m=1), the material is said to be ideally superplastic. In actuality, maximum superplastic ductilities are usually obtained at the strain rate corresponding to the maximum value of the strain rate sensitivity coefficient, m, and the value of m strongly depends on the characteristics of the microstructure developed through the thermomechanical process [Ref. 14].

The most common utilized technique of achieving high m values in aluminum alloys is by grain size refinement, obtained by thermomechanical processing. Values of grain size less than 10μm are considered a requirement for superplastic behavior, and typical corresponding m values of superplastic materials range from 0.4 - 0.5 [Ref. 2]. The shape of the grains is also an important factor in superplastic behavior. Equiaxed, fine grains allow grain boundaries to slide, rotate, and thus preclude local stress build-up which could, in turn, promote cavitation and lead to failure.

The flow stress-strain rate relationship is very sensitive to grain size, and superplastic materials can be grouped into those exhibiting a rate proportional to d^{-2} and those to d^{-3}, where d is the grain size. At a given constant stress, the strain rate increases, therefore, with a decrease in grain size [Ref. 7].

It has been shown that the activation energy for superplastic flow is equal to that for grain boundary diffusion, and, for some fine-structures, equal for lattice self-diffusion [Ref. 7]. This can be understood in terms of an effective diffusion coefficient. The effective diffusion coefficient is equal to the sum of the diffusion coefficients of lattice diffusion and grain boundary diffusion.

$$D_{eff} = D_L f_L + D_{gb} f_{gb} \qquad \textbf{Equation 6}$$

where f_L and f_{gb} are the fractions of atoms associated with lattice and grain boundary diffusion respectively. Typically $f_L=1$ and $f_{gb}=(\pi \times w)/d$, where w is the grain boundary width and d is the grain size. Rewriting equation 6 yields:

$$D_{eff} = D_L + D_{gb}\left(\frac{\pi w}{d}\right) \qquad \textbf{Equation 7}$$

As d decreases below some vale, the grain boundary term will begin to predominate and this demonstrates that either grain boundary or lattice diffusion can control deformation depending upon d and the deformation temperature. The grain size, stress-strain rate relationship has been reported as having the form:

$$\dot{e} \;\alpha\; \left(\frac{D_{eff}}{d^2}\right) f\,(\sigma/E) \qquad \textbf{Equation 8}$$

where $f(\sigma/E) = (\sigma/E)^2$. Equation 8 predicts a strain rate sensitivity coefficient m=0.5 and either lattice or grain boundary diffusion control depending on the grain size.

At superplastic deformation temperatures grain size is not stable. Strain rate dependent grain growth may occur, resulting in a strain dependent m value. Previous TMPs have resulted in partially recrystallized structures that exhibited moderate superplastic responses. In this research, previous rolling schedules will be modified to incorporate larger strains. It is anticipated that a matrix, containing uniformly distributed, critically sized particles, and deformed at higher strain values will be more responsive to PSN and ultimately transform into a fine structure-ideally one grain per particle.

III. EXPERIMENTAL PROCEDURE

A. MATERIAL

The Alcoa Technical Center, Alcoa Center, Pennsylvania, provided a direct-chill cast ingot, designated S572826, which had a nominal composition Al-10Mg-0.1Zr (wt%) [Ref. 15]. The ingot measured 6 in. diameter x 23 in. length (150 mm dia x 580 mm length). The complete chemical composition of the alloy is presented in Table II.

TABLE II. NOMINAL ALLOY COMPOSITION (wt%)

CASTING	Mg	Zr	Si	Fe	Ti	Be	Al
S572826	9.89	0.09	0.02	0.02	0.01	0.003	Balance

The ingot was sectioned into billets measuring 3.75 in x 1.25 in x 1.25 in (93.5 mm x 31.8 mm x 31.8 mm). The billets were cut with their greatest dimension parallel to the longitudinal direction of the ingot.

B. THERMOMECHANICAL PROCESSING

Thermomechanical processing (TMP) consists of two phases: solid solution treatment/hot working, and the warm rolling. Figure 2 displays the general TMP schedule followed. The billets were initially homogenized in a Lindberg Furnace,

model 51828, at 440°C, a temperature below the eutectic temperature of 451°C, for 6 hours. Homogenization was followed by a solid solution treatment, which was conducted for 18 hours at 480°C.

Following the solution treatment, the billets were upset forged along their long direction thickness to 1 inch (25.4mm) +/- .0055 inches (.1397 mm) on a Baldwin-Tate-Emery testing machine with platens heated to 440°C. The forged billets were then resolutionized at 480°C for one hour to ensure subsequent quenching was done from above the solvus temperature. The fully solid solution treated billets were then given a vigorous oil quench for one minute and transversely cut in half to facilitate warm rolling.

The second part of the TMP consists of warm rolling at a temperature of 300°C, a temperature well below the β phase solvus temperature of 360°C. A Blue M Electric Co. box type furnace, model 86553 was used to anneal the forged billets. A steel plate was utilized as a heat sink to obtain near isothermal conditions, and three K type (Chromel and Alumel) thermocouples (+/- 1°C) were positioned along the plate to monitor the temperature. Forged billets were annealed at 300°C for 30 minutes prior to rolling. Tables III, IV, and V represent the rolling schedules that were followed. A Fenn Laboratory rolling mill, with roll diameter of 4.0 inches rotating at .327 rads/sec, was used. The desired mill gap was set by hand and checked by gage blocks and a feeler gage. Strain calculations required accounting for the mill's deflection, which was estimated to be .033 inches per pass. Mill gap setting was accurate to about +/- .001 in. At the

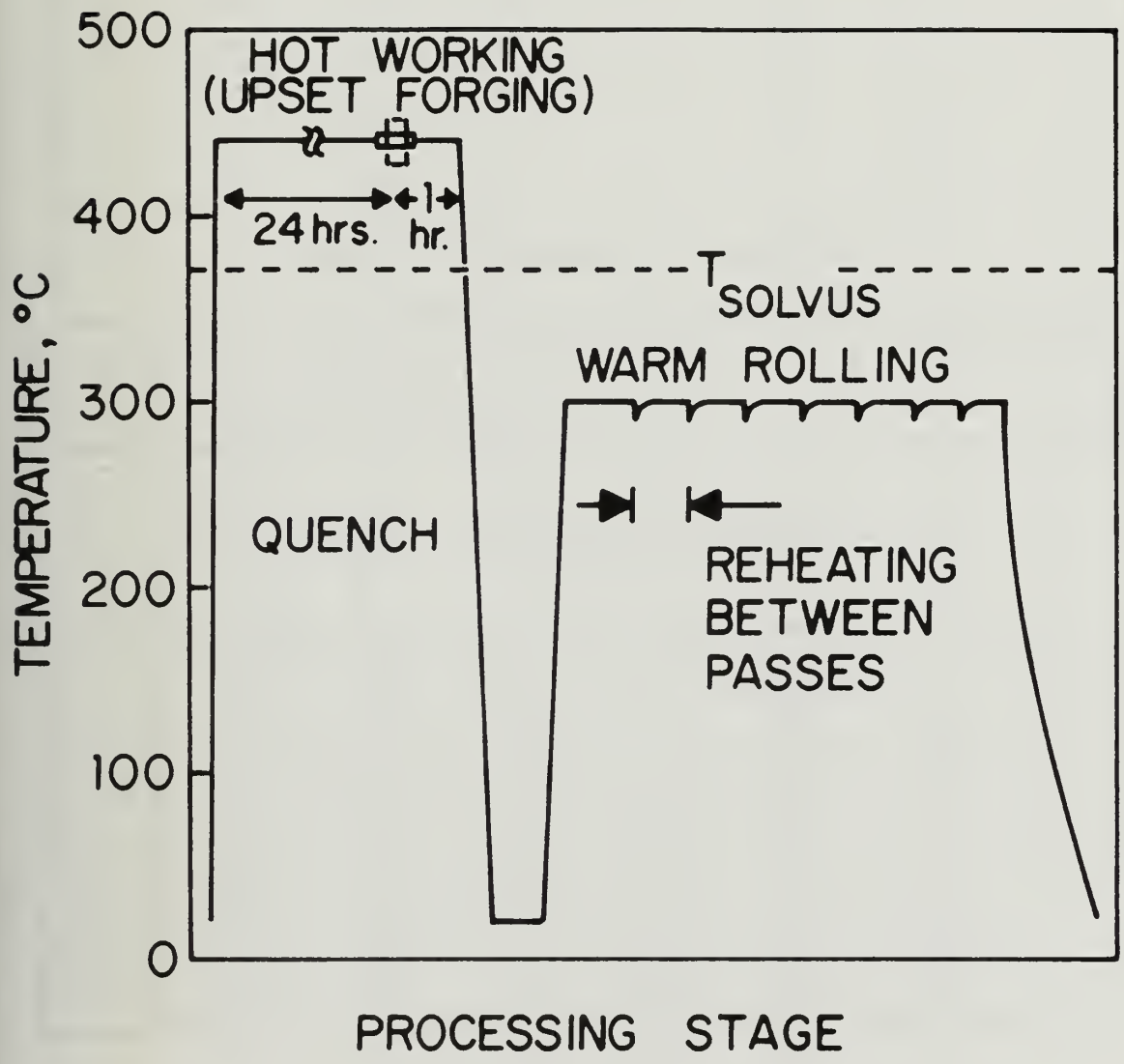

Figure 2. General TMP Schematic.

conclusion of each pass the material's thickness was measured with a digital micrometer and the billet promptly returned to the furnace. The rolling process from the time the specimen left the furnace to it's return was less than 15 seconds. Figures 3, 4, and 5 show the calculated versus actual strains achieved for each TMP.

TABLE III. TMP 6 ROLLING SCHEDULE

PASS	MILL GAP (in)	H_i (in)	H_f (in)	ΔH (in)	MILL DEFLECTION (in)	ε (%)	$\dot{\varepsilon}$ sec^{-1}
1	0.900	1.008	0.928	0.080	0.028	7.94	0.83
2	0.790	0.828	0.821	0.107	0.031	11.53	1.05
3	0.680	0.821	0.723	0.098	0.043	11.94	1.14
4	0.570	0.723	0.607	0.116	0.037	16.04	1.42
5	0.460	0.607	0.493	0.114	0.033	18.78	1.69
6	0.350	0.493	0.388	0.105	0.034	21.30	2.01
7	0.265	0.388	0.299	0.089	0.034	22.94	2.36
8	0.195	0.299	0.229	0.070	0.034	23.41	2.72
9	0.140	0.229	0.174	0.055	0.034	24.02	3.15
10	0.100	0.821	0.133	0.041	0.033	23.56	3.58
11	0.070	0.133	0.102	0.031	0.032	23.41	4.07
12	0.047	0.102	0.080	0.022	0.033	21.57	4.45
13	0.025	0.080	0.055	0.025	0.030	31.25	6.19

TABLE IV. TMP 7 ROLLING SCHEDULE

PASS	MILL GAP (in)	H_i (in)	H_f (in)	ΔH (in)	MILL DEFLECTION (in)	ε (%)	$\dot{\varepsilon}$ sec^{-1}
6	0.900	1.008	0.929	0.079	0.028	7.84	0.83
7	0.790	0.929	0.816	0.113	0.026	12.16	1.08
4	0.680	0.816	0.708	0.108	0.028	13.24	1.21
4	0.570	0.708	0.598	0.816	0.028	15.54	1.41
5	0.460	0.598	0.489	0.109	0.031	18.23	1.68
4	0.350	0.489	0.380	0.109	0.030	22.29	2.07
7	0.265	0.380	0.296	0.084	0.031	22.11	2.34
8	0.195	0.296	0.225	0.071	0.030	23.99	2.07
6	0.140	0.225	0.173	0.052	0.033	23.11	3.11
10	0.100	0.173	0.134	0.039	0.034	22.54	3.50
11	0.070	0.134	0.104	0.030	0.034	22.39	3.97
12	0.035	0.104	0.069	0.035	0.034	33.65	5.67

TABLE V. TMP 8 ROLLING SCHEDULE

PASS	MILL GAP (in)	H_i (in)	H_f (in)	ΔH (in)	MILL DEFLECTION (in)	ε (%)	$\dot{\varepsilon}$ sec^{-1}
6	0.850	1.024	0.896	0.128	0.046	12.50	1.05
7	0.750	0.896	0.784	0.112	0.034	12.50	1.12
3	0.850	0.784	0.688	0.096	0.031	12.24	1.18
6	0.580	0.688	0.609	0.079	0.029	11.48	1.22
5	0.515	0.609	0.546	0.063	0.031	10.34	1.23
6	0.430	0.546	0.457	0.089	0.028	16.30	1.68
7	0.338	0.452	0.354	0.103	0.016	22.54	2.16
6	0.220	0.354	0.256	0.098	0.036	27.68	2.75
9	0.112	0.256	0.162	0.094	0.050	36.72	3.80
10	0.040	0.162	0.090	0.072	0.050	44.44	5.35

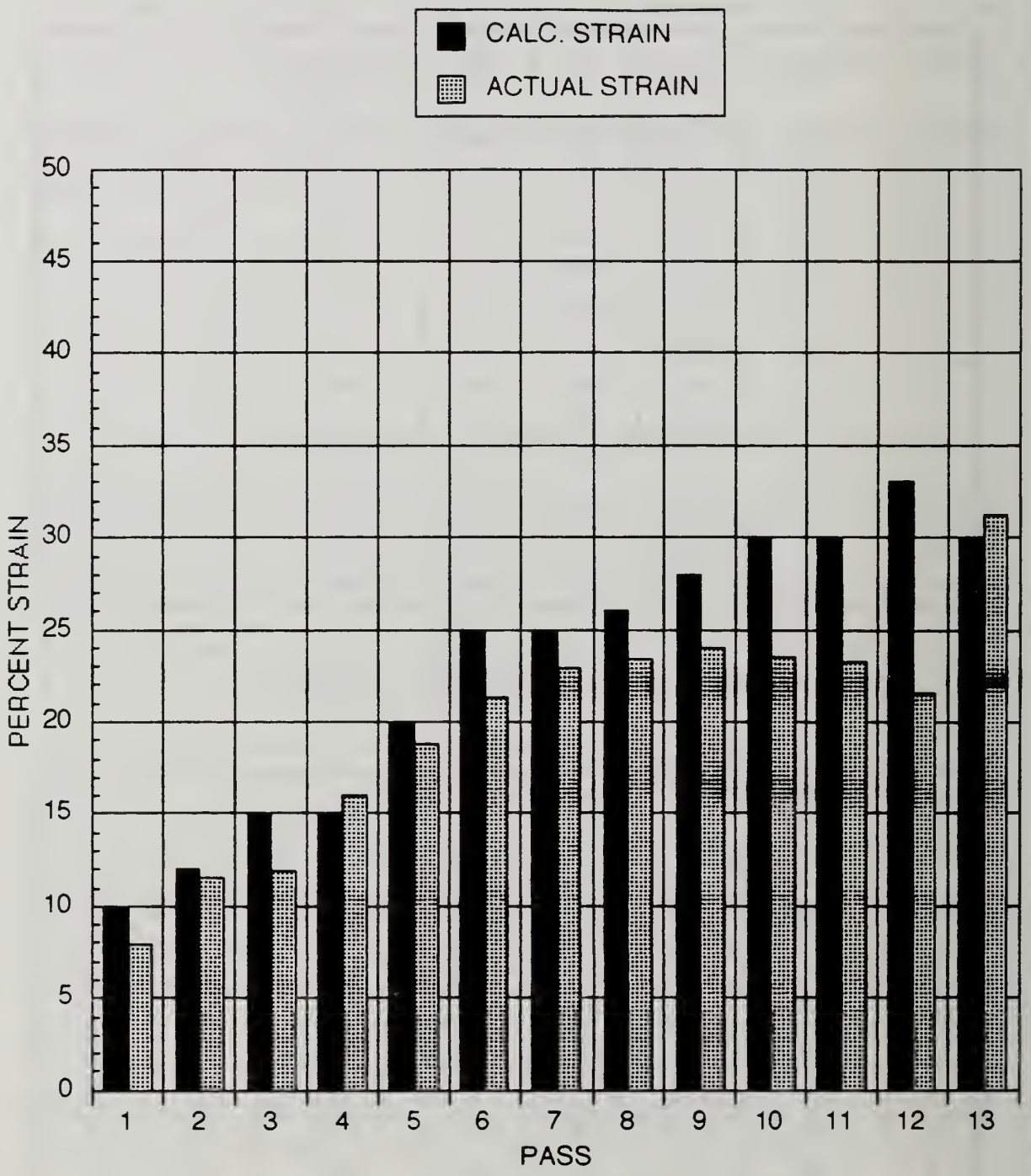

Figure 3. Calculated and Actual Strains for TMP 6.

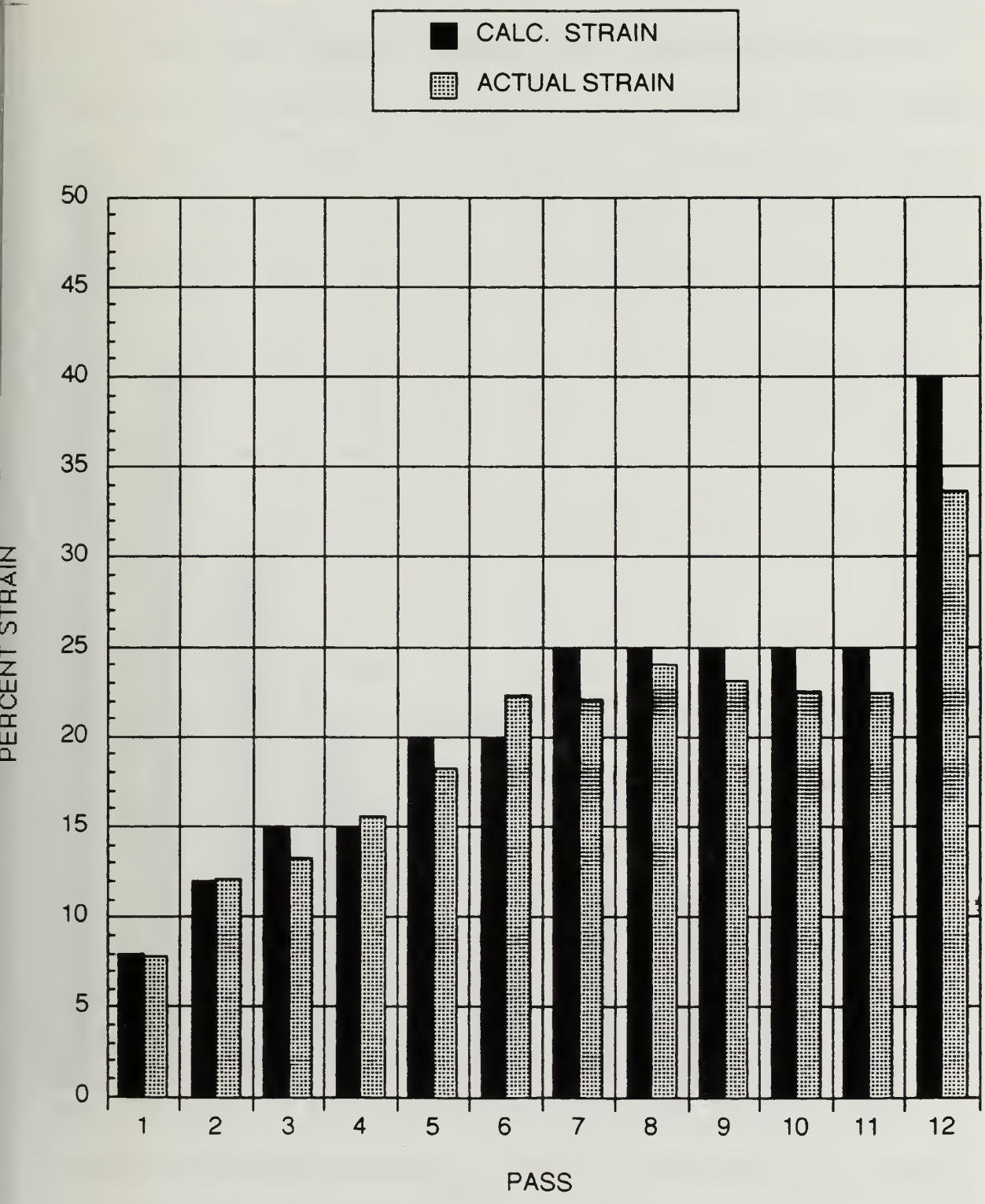

Figure 4. Calculated and Actual Strains for TMP 7.

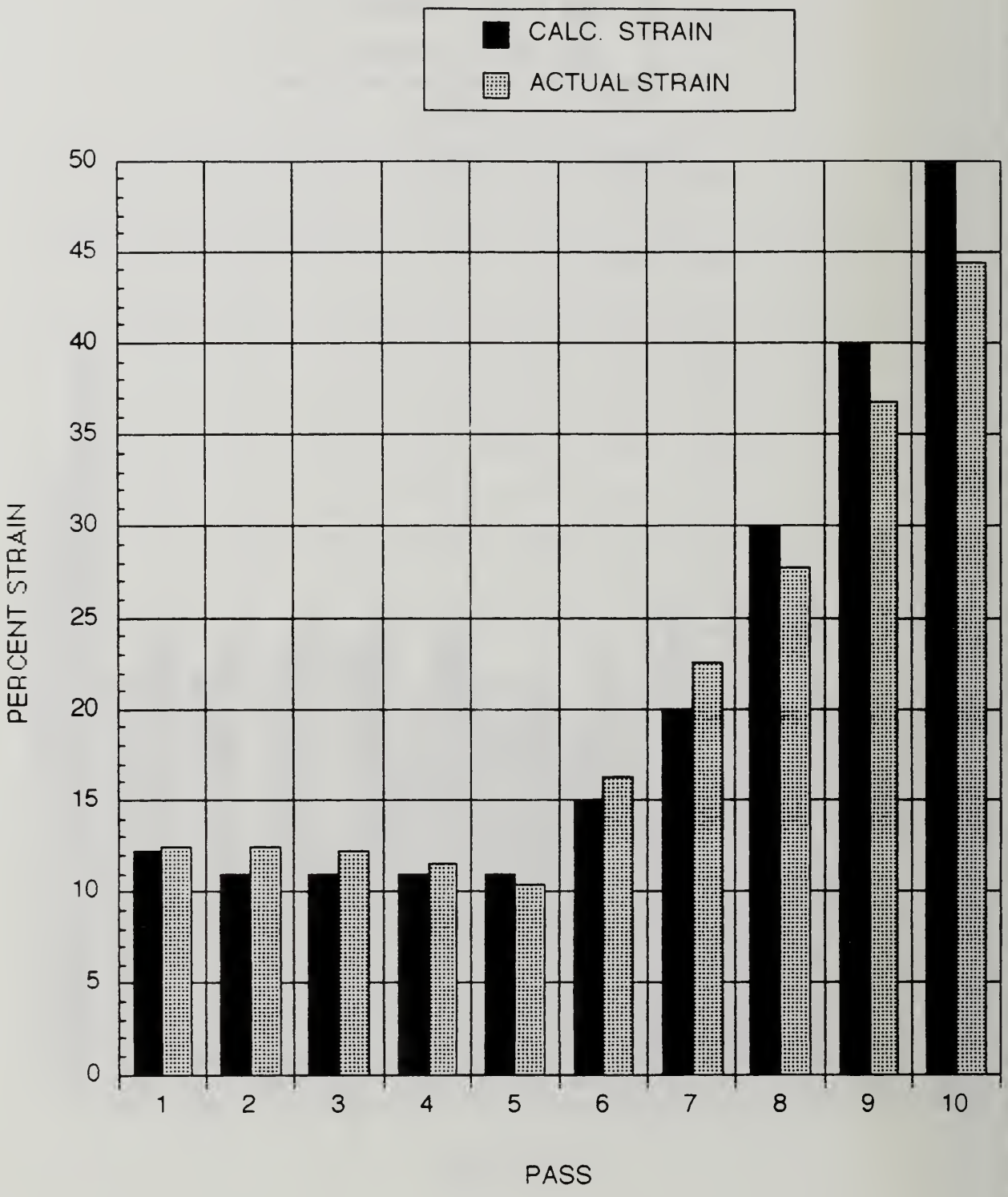

Figure 5. Calculated and Actual Strains for TMP 8.

Between passes, post roll annealing was conducted for 30 minutes at 300°C. To ease the frictional forces encountered in the later passes of rolling, silicone spray lubricant was applied to the rolls prior to the 6th pass and prior to subsequent passes for each TMP series. After completion of the TMP, the rolled sample was quenched in water, and sections were cut from the ends. On one of the sectioned ends, a post-roll 30-minute anneal at the rolling temperature was conducted for future microscopic and mechanical (hardness) comparisons with the as-rolled specimens. The remaining bulk of the as rolled material was submitted for tensile test coupon manufacturing according to the specifications shown in Figure 6.

C. HARDNESS TESTING

Hardness testing was conducted on the as-rolled and annealed samples. A Rockwell Hardness stand and 1/16th inch diameter ball penetrator were used. A series of eight to ten tests per specimen were conducted and averaged.

D. MECHANICAL TESTING

Tensile testing was conducted on an Instron Model 6027 testing machine utilizing a 200 KN load cell. A Marshall Model 1134 tubular furnace (110 Volts,14.11 Amps, 1.6 KVA) provided the elevated test condition of 300°C. A Eurotherm, Model 808 temperature controller set and monitored the temperature of the furnace.

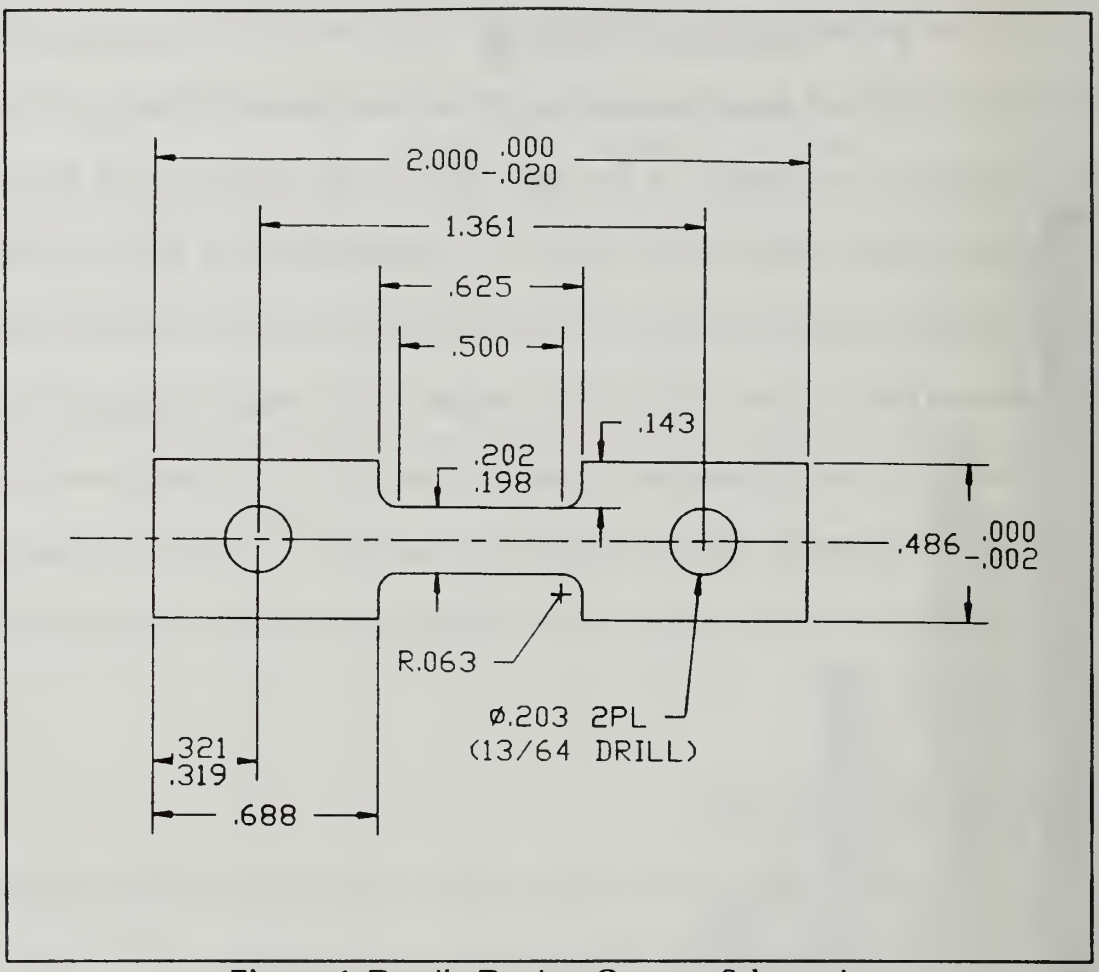

Figure 6. Tensile Testing Coupon Schematic.

Initially, three K type thermocouples were positioned along the cage assembly that corresponded to the top, middle and bottom sections of the test specimen. Typical thermal gradients of 15 degrees along the specimen length resulted and were deemed excessive.

The Marshall Model 1134 tubular furnace consists of a single, continuous wound heating coil that has external shunting posts positioned along its length. Model 1134 has ten shunt posts spaced approximately 1.75 inches apart, resulting in nine controllable heat zones. Seven additional thermal couples were placed

along the cage assembly, using the positions of the shunt posts on the furnace as reference points. Shunting was conducted in accordance with the manufacturer's guidelines, but the results were inadequate. Individual zones that were shunted had an overall reduced thermal gradient, but the inability to reduce the thermal gradients between neighboring zones persisted. Overall, the thermal gradient along the test sample length was reduced to 8°C above the set point of 300°C, but adjacent heat zones' thermal gradients exceeded 20 degrees.

Samples to be tensile tested were placed in preheated grips (150°C) and placed in the cage/furnace assembly. The sample was allowed 50 minutes to come to the test temperature of 300°C. The lowest available range for the load cell of 2 KN was selected. Two crosshead speeds of 0.02 and 0.2 in/min (.508 and 5.08 mm/min), which corresponded to strain rates of 6.67×10^{-3} and 6.67×10^{-4}, were used. Samples were pulled to failure and elongation measured with a digital micrometer.

E. DATA REDUCTION

The following data was obtained from each tensile test: time (min), load (KN), crosshead position (mm), engineering stress (MPa) and strain (%). A graph of load versus position or displacement was constructed. This data was corrected to account for the tightening of the grips under the initial load, the elastic response of the testing machine and the different crosshead speeds used. [Ref. 11]. The correction allows the data to be directly compared. The corrected data was

then converted to a plot of true stress versus true strain. Values for true stress taken at calculated true strain of 0.1 were then plotted on double log axes versus strain rate to determine the strain rate sensitivity coefficient, m.

F. SCANNING ELECTRON MICROSCOPY

Backscattered imaging technique was used to study the microstructures of the as-rolled and the annealed conditions, particularly the nature of deformation bands and recrystallized grains. [Ref. 16] discusses the application and the result of using such a technique to enhance the orientation contrasts which aid in the explanation of the conversion process of a fine grained microstructure by PSN.

The end portions cut from the as-rolled sheets and the post annealed material were viewed and studied in a Cambridge Model S200 scanning electron microscope. The desired area to be studied was the short-longitudinal plane shown in Figure 7.

Material was cut to desired size on a diamond cutting wheel, ground flat successively on 240, 320, 400, and 600 grit sandpaper, and polished to a mirror finish using 1.0 micron diamond paste. Following mechanical polishing, the samples were electropolished using a solution of 90% Butoxyethanol- 10% hydrochloric acid at 0°C. A voltage of 16 VDC was applied for three minutes, and the resulting amperage varied from .02 to .04 amps. The final prepared samples were then mounted with graphite conducting paint. Tungsten and LaB6 filaments

were utilized on the scanning electron microscope, and were operated at a voltage potential of 20kV and 25kV, respectively.

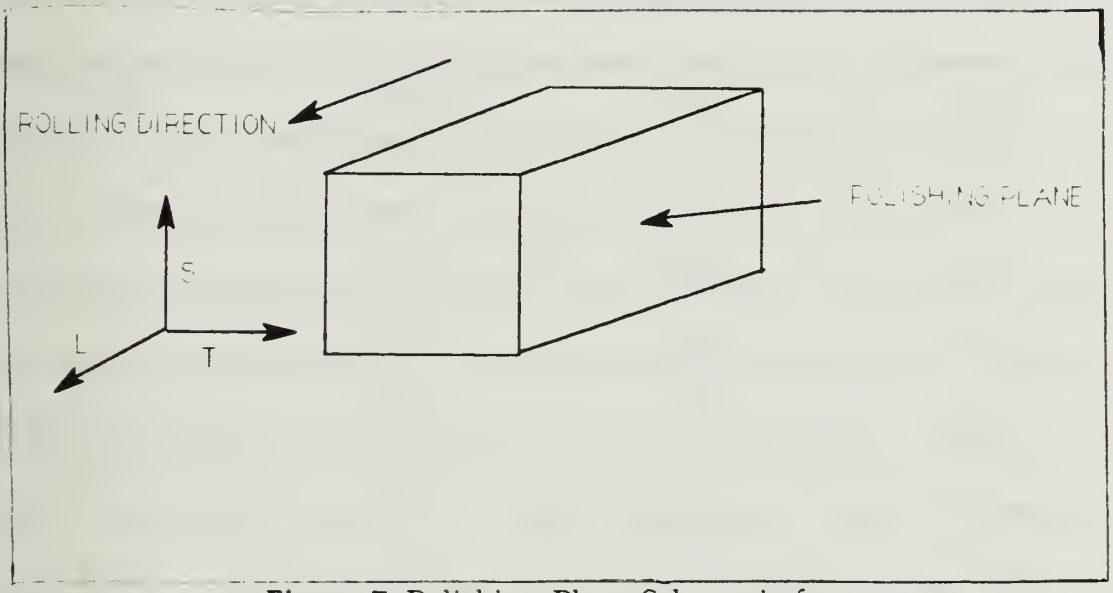

Figure 7. Polishing Plane Schematic for Scanning Electron Microscope.

IV. RESULTS AND DISCUSSION

A. PROCESSING RESULTS

Three rolling schedules designated as TMP 6, TMP 7, and TMP 8 were developed for the studies and are detailed in Tables III, IV, and V respectively. TMP 6 is similar to the rolling schedules utilized previously [Ref. 8.], except that no samples were sectioned from the rolled sheets after various intermediate passes. For TMP 7, the primary modification made from the TMP 6 rolling schedule was that a larger strain was attained in the last pass by alternating the sequence of reductions to reduce the strains in the earlier passes. For TMP 8, two fewer passes were used and smaller strains in the intermediate passes were employed in order to accommodate larger strains in the later passes. All three schedules were designed to provide reductions corresponding to a total strain of 2.5. Also of note is that for all three developed schedules the strain rate increases on each successive pass.

Figures 3, 4, and 5 present both the calculated and actual, measured strains obtained on each pass for TMPs 6, 7, and 8. The difficulty in attaining agreement between calculated and actual strains for each pass is the inability to accurately predict mill deflection with the laboratory rolling mill used. From previous rolling operations of similar material and schedules, an average mill deflection of 0.033

inches was taken into account in developing the rolling schedules. For TMP 7 and 8 this estimation proved more accurate than for TMP 6. Table VI directly compares the strain per pass of the three TMPs. For one sample, an additional thirteenth pass was made on a portion of the material processed according to TMP 6 in order to make microscopic comparisons with TMP 7.

TABLE VI. STRAIN PER PASS COMPARISON OF TMP 6, 7, 8

PASS	TMP 6	TMP 7	TMP 8
1	7.94	7.84	12.50
2	11.53	12.16	12.50
3	11.94	13.24	12.24
4	16.04	15.54	11.48
5	18.78	18.23	10.34
6	21.30	22.29	16.30
7	22.94	22.11	22.54
8	23.41	23.99	27.68
9	24.02	23.41	36.72
10	23.56	22.54	44.44
11	23.31	23.39	
12	21.57	33.65	
13	31.25		

B. HARDNESS TEST RESULTS

Rockwell Hardness testing was conducted on samples representative of these TMPs, both in the as-rolled condition and following 30 minutes of annealing at the conclusion of these schedules. The hardness data from as-rolled specimens correspond directly to the effect of the rolling process, while hardness obtained from the annealed specimens correspond to material immediately preceding tensile testing. In all cases, a 1/16th inch ball indentor, and a major load of 100 KN were used and eight to ten "B" scale readings were recorded and averaged.

Table VII contains the hardness results for material processed according to each of TMP 6, 7 and 8. The hardness value for each condition is not proportional to the accumulated strain during the rolling process. For example, material processed by TMP 6 at the conclusion of pass 13 has an accumulated strain of 2.9 and a corresponding hardness value of HRB 75.8, while TMP 8 at the conclusion of pass 10 has an accumulated strain of 2.4, yet a hardness value of HRB 81.2. The hardness values are more reflective of the strain attained at the last pass of the TMP. The last pass for TMP 6 (12 & 13 pass samples) and also TMPs 7 and 8, had final strains of 0.22, 0.31, 0.34, and 0.44 respectively. From the table, the aforementioned have increasing hardness values of HRB 71.5, 75.8, 77.0, and 81.2 corresponding to these increasing strains.

TABLE VII. HARDNESS VALUES FOR AS-ROLLED & ANNEALED CONDITIONS FOR TMP 6, 7, 8

SCHEDULE	STRAIN ACCUM.	STRAIN (LAST PASS)	HARDNESS AS ROLLED	HARDNESS 30 MIN ANN	Δ HARDNESS
TMP 6					
12 PASS	2.5	21.57	71.8	50.7	21.1
13 PASS	2.9	31.25	75.8	44.4	31.4
TMP 7	2.7	33.65	77.0	55.8	21.2
TMP 8	2.4	44.44	81.2	54.8	26.4

The hardness values for the annealed specimens, as well the difference between the as-rolled and annealed values, are also included. Of interest is that neither the annealed hardness value nor the difference between as-rolled and annealed hardness is an indication of the amount of recovery and/or recrystallization that has occurred. Previous microstructural observations of material processed by TMP 8 and then annealed, which has a hardness value of 54.8, indicates a fully recrystallized condition, while observations of the structure of material processed by TMP 6 (after 12 passes) indicates only partial recrystallization, yet the hardness value is 50.7.

Hardness testing was also conducted on material sectioned following various passes (3, 6, 8, 10, 12) in previous processing for TMP 6. Figure 8 graphically shows the as-rolled and annealed hardness values plotted versus pass number. The as-rolled hardness values increase monotonicallay with successive passes (strain), while the annealed hardness values also increase until the last measurement where the hardness value decreases. This may indicate that

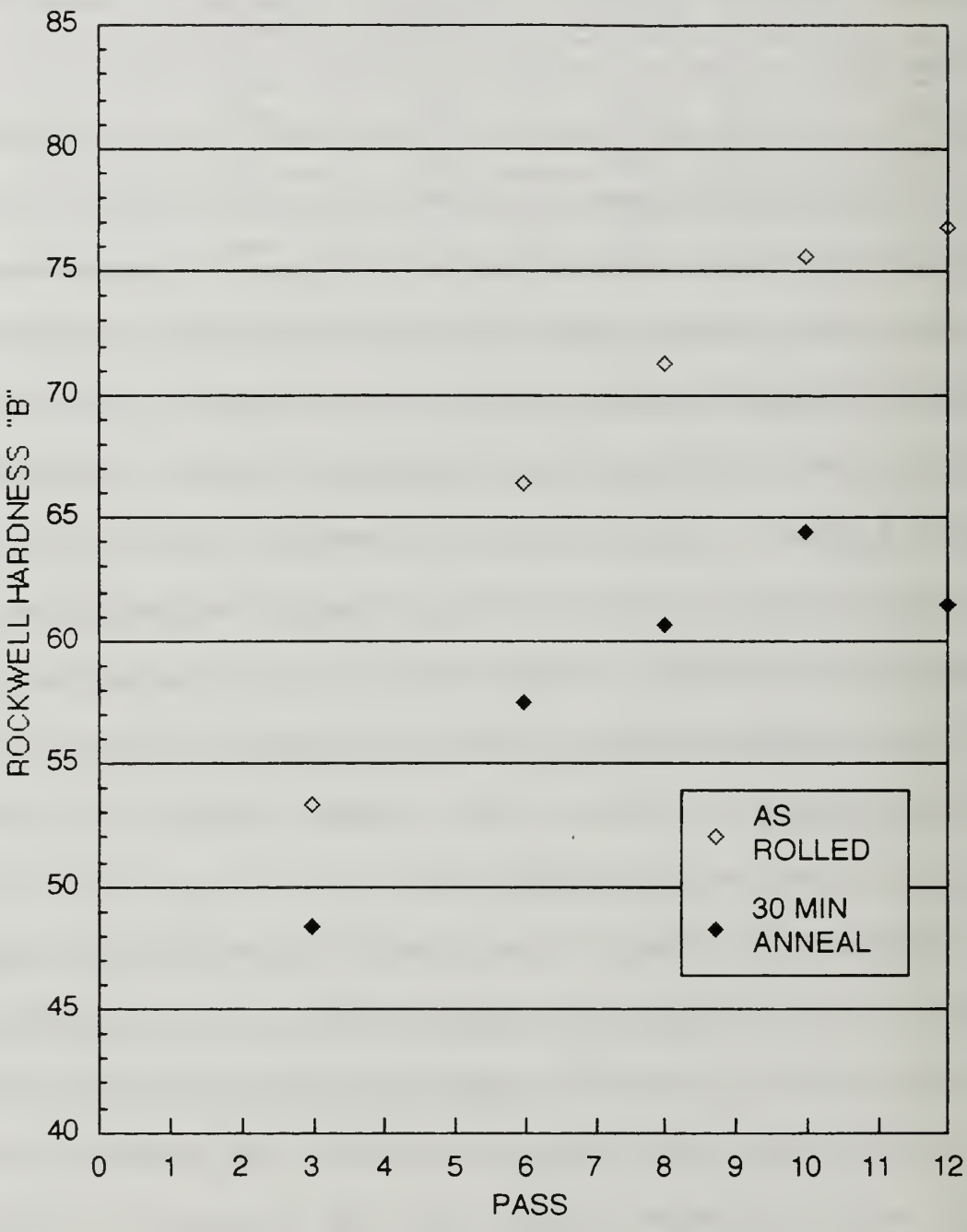

Figure 8. Hardness versus Rolling Pass for TMP 6.

recovery has further progressed to recrystallization but, again, not an indication of the amount of recrystallization.

C. MICROSCOPY

Using backscattered imaging on the scanning electron microscope, the microstructures of the Al-10Mg-0.1Zr alloys were analyzed. Samples representing the as-rolled and annealed conditions for the various TMP schedules (TMP 6, TMP 7 and TMP 8) were examined. For any pair of as-rolled and annealed samples, the only processing difference upon annealing is the additional time at temperature (30 minutes at 300°C). The as-rolled sample is indicative of the microstructure at the completion of the TMP, while the annealed sample is more indicative of the microstructure prior to tensile testing.

Other microstructures to be analyzed included those from intermediate passes of TMP 6 as previously processed. At the conclusion of various intermediate passes (3, 6, 8, 10) samples were sectioned from the rolled sheets prior to their being returned to the furnace. When samples were cut, the amount of time the rolled sheet was out of the furnace was approximately 45 seconds [Ref. 10], compared to only 15 seconds when no samples were cut. The microscopic analysis of TMP 6 for the various successive passes will provide further insight into the final processed microstructure of this alloy.

1. TMP 6

The microstructure of the as-rolled condition after pass 3 is shown in Figure 9a. The microstructure reveals precipitation of the intermetallic β phase on prior grain boundaries. Non-uniform dispersion of the precipitates within the grain interior is clearly present. Precipitation appears to be occurring on deformation structures formed due to straining. Figure 9b represents the annealed structure after pass 3. Due to additional time at temperature, the β particles have coarsened and appear to be more uniformly dispersed as further precipitation has occurred.

Figure 10a shows the microstructure for the as-rolled condition at the conclusion of pass 6. Clearly, additional precipitation has occurred since pass 3, as evident by smaller particles present within the matrix. Particles that had previously precipitated on prior grain boundaries have coarsened. Indications of recovery are shown by local contrast differences indicative of orientation differences in the structure. Figure 10b shows the microstructure for the annealed condition after pass 6. Particle growth for both newly and previously precipitated particles appears to have occurred, and a more uniform distribution of the particles is also apparent. Recovery is clearly evidenced by the orientation contrast differences in regions of high particle content. Previous grain boundaries are still evident, but the particles have both grown and become separated by deformation bands. Figure 10c is this same annealed condition but at a higher magnification. Of particular note is the fine equiaxed substructure regions containing particles.

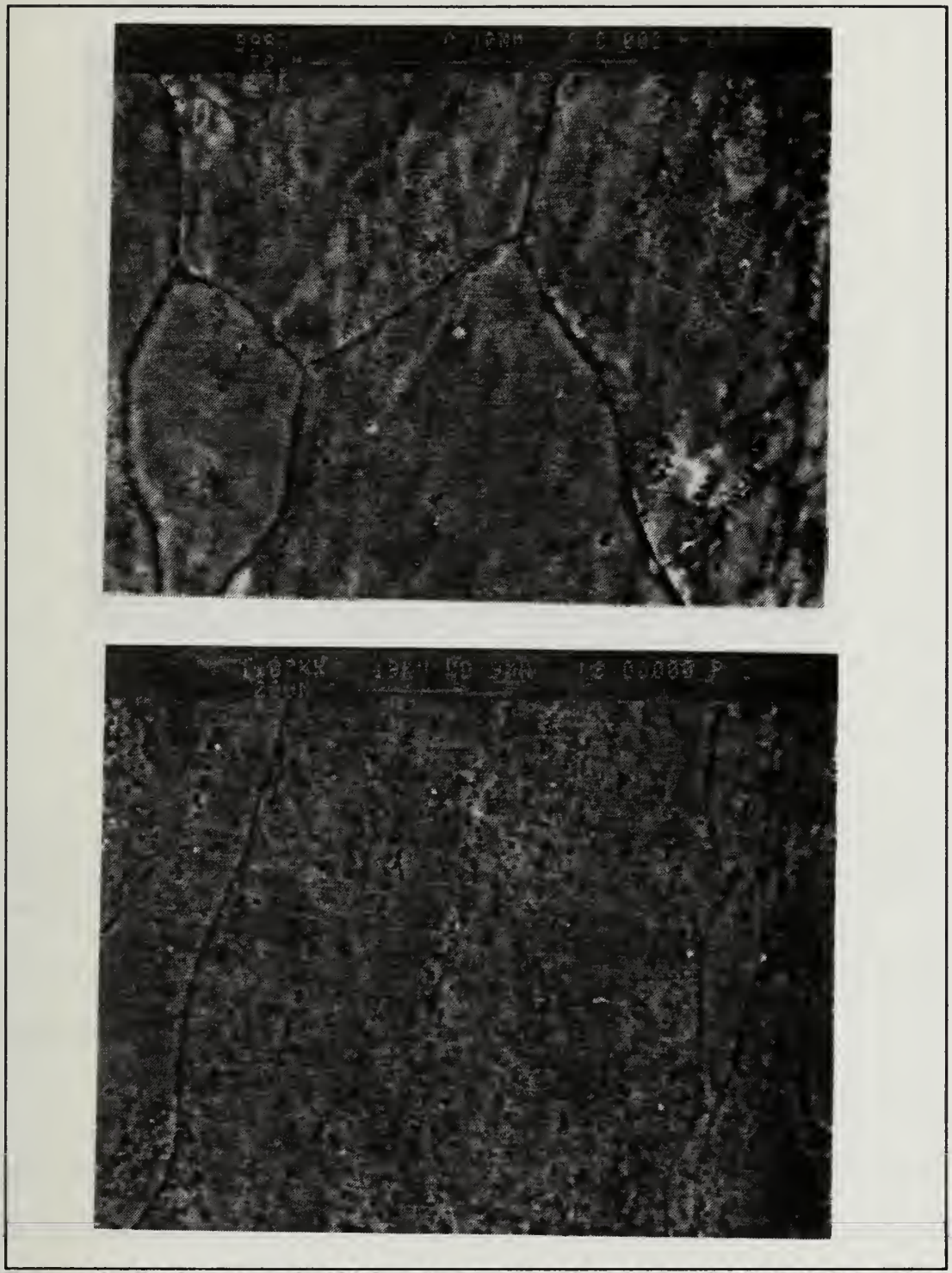

Figure 9. Backscattered SEM micrograph showing Al-10Mg-0.1Zr alloy following pass 3 of TMP 6: a) in the as-rolled condition; b) following 30 minutes of annealing at 300°C.

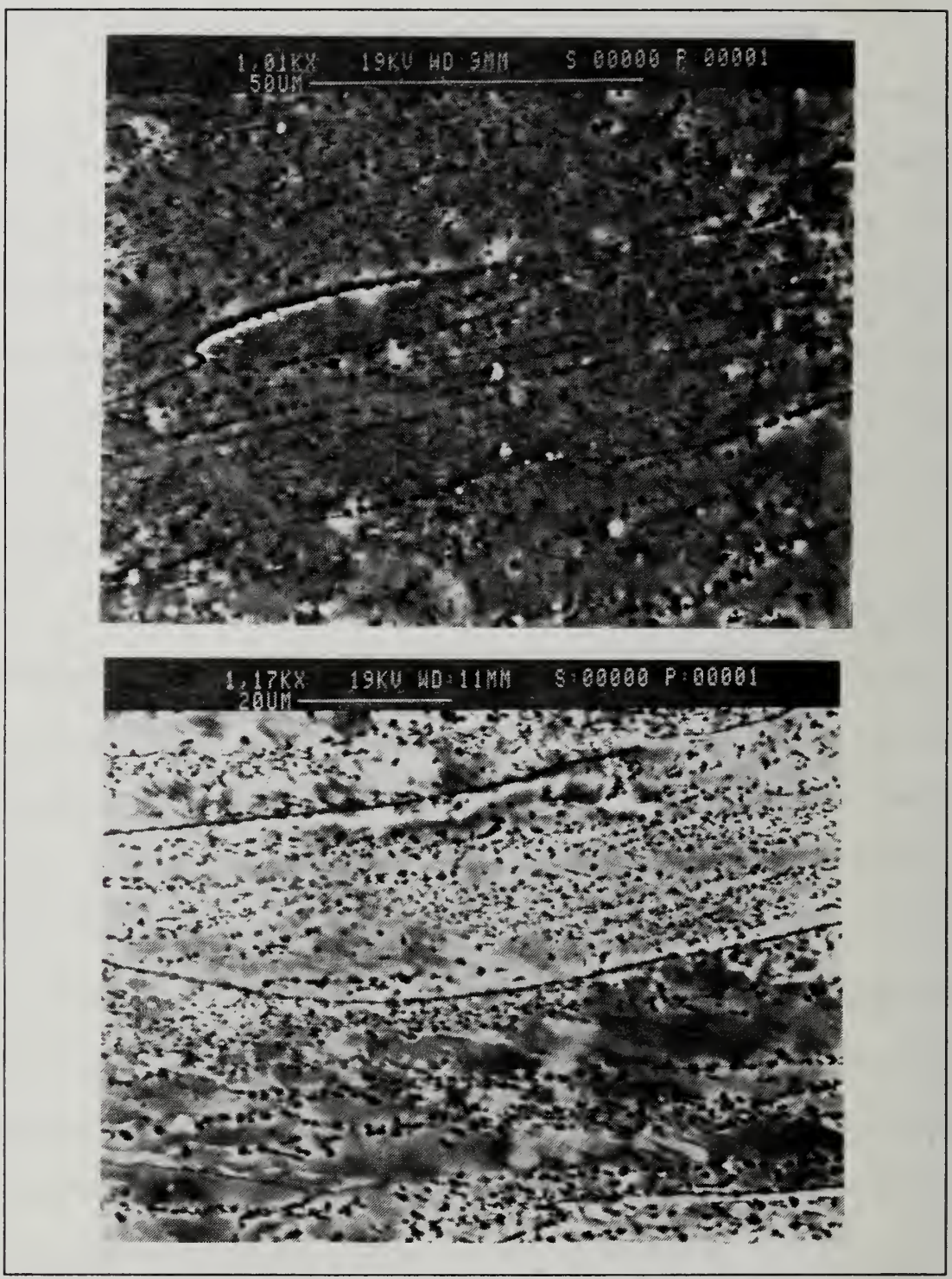

Figure 10. Backscattered SEM micrograph showing Al-10Mg-0.1Zr alloy following pass 6 of TMP 6: a) in the as-rolled condition; b) following 30 minutes of annealing at 300°C.

Figure 10. Backscattered SEM micrograph showing Al-10Mg-0.1Zr alloy following pass 6 of TMP 6: c) in the annealed condition at a higher magnification.

Elsewhere, elongated deformation bands also show evidence of recovery but also coarser structures are apparent.

The as-rolled condition following pass 8 is shown in Figure 11a. The precipitation of β phase from solid solution likely has concluded prior to this pass. Instead, particles have coarsened further, and recovered areas throughout the structure are more pronounced as clearly shown by orientation contrast. Around larger precipitates are areas of contrast variation suggesting local lattice

orientation variation characteristic of deformation zones. Figure 11b represents the structure for the annealed condition following pass 8. Figure 11c is the same annealed structure but at a higher magnification. In both cases, evidence of early stages of particle stimulated nucleation in areas that contain larger particles is evident. In such areas, larger recovered areas indicated by lighter contrast have developed since pass 6.

Figure 12a represents the microstructure of the as-rolled condition for the completed TMP 6 (pass 12). The β phase has fully precipitated and the β particles have become uniformly dispersed throughout the matrix. In the regions where particles have coarsened, recovery is evident. Figure 12b is the annealed condition. Recrystallization is apparent as seen by new grains outlined by sharply contrasted grain boundaries. The material is only partially recrystallized for recovered areas are still present.

2. TMP 7

The as-rolled condition following the final pass for TMP 7 is shown in Figure 13a. Compared with the as-rolled condition of TMP 6, the TMP 7 microstructure exhibits β particles that are coarser, but more uniformly distributed throughout the matrix. There is also more evidence of recovery in the matrix. The major differences between the two processes is the strain in the last pass and the accumulated strain at the conclusion of the TMP. For TMP 6, the strain of the last pass was 0.22, with an accumulated strain of 2.5. For TMP 7, the strain of pass 12 was 0.34 and the accumulated strain of 2.7. Figure 13b represents

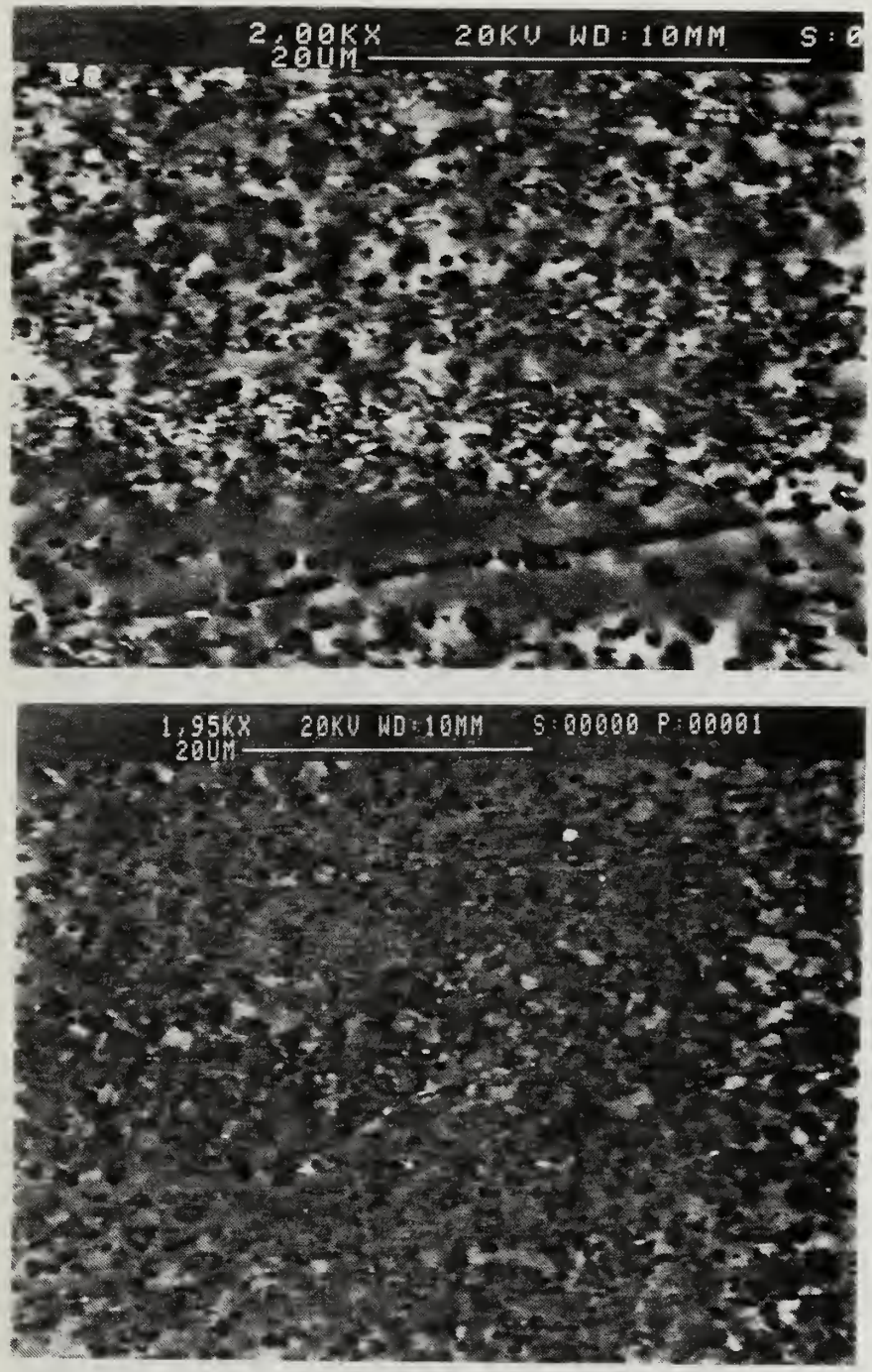

Figure 11. Backscattered SEM micrograph showing Al-10Mg-0.1Zr alloy following pass 8 of TMP 6: a) in the as-rolled condition; b) following 30 minutes of annealing at 300°C.

Figure 11. Backscattered SEM micrograph showing Al-10Mg-0.1Zr alloy following pass 8 of TMP 6: c) in the annealed condition at a higher magnification.

the microstructure for the annealed condition following the last pass (pass 12) of TMP 7. Compared to Figure 12b (TMP 6, pass 12, annealed condition), the microstructure appears to be completely recrystallized. Sharp contrast between recrystallized grains with sharply defined grain boundaries can be seen. Figure 13c shows at a higher magnification the orientation contrast associated with the recrystallized grains.

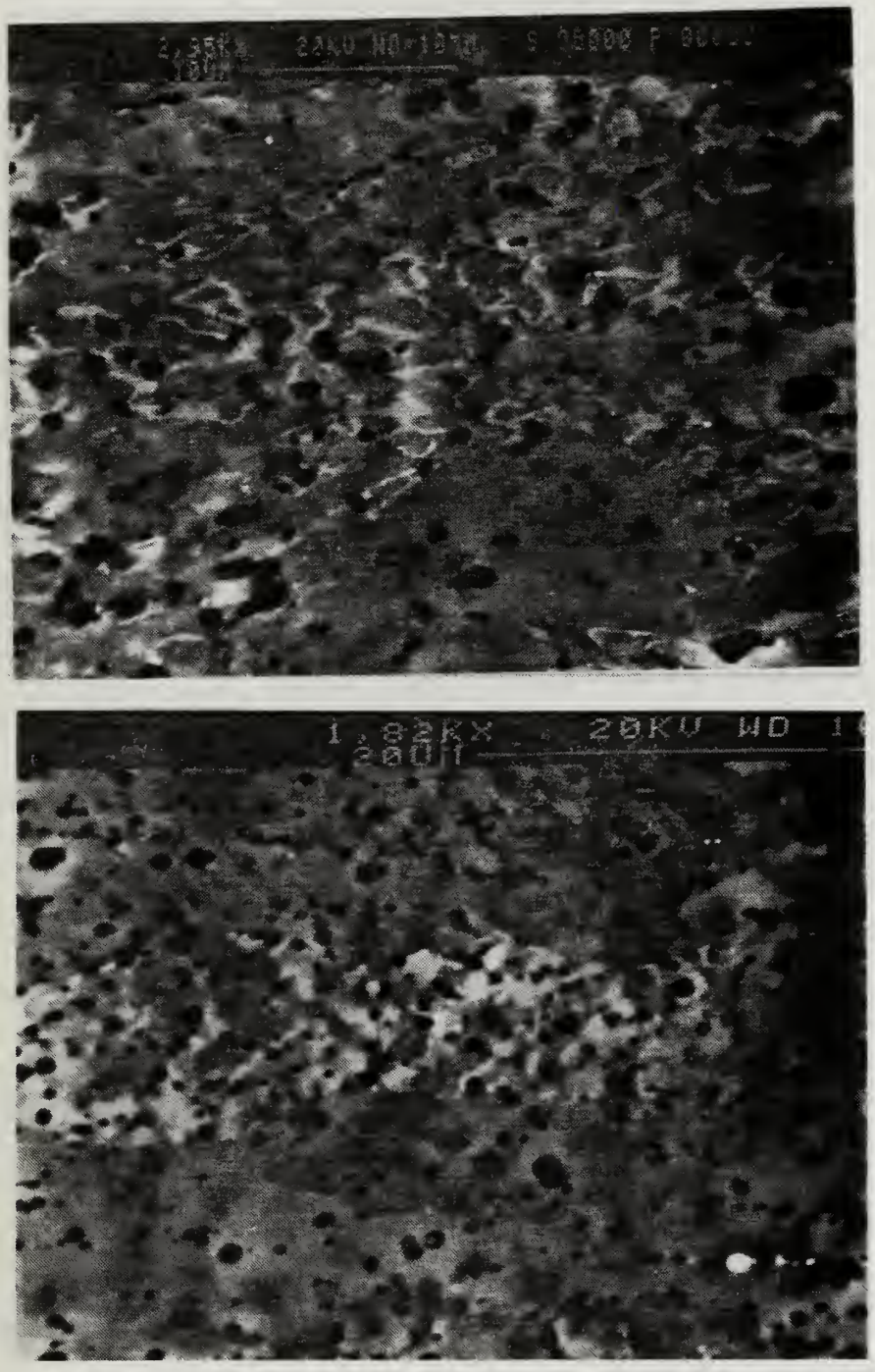

Figure 12. Backscattered SEM micrograph showing Al-10Mg-0.1Zr alloy following pass 12 of TMP 6: a) in the as-rolled condition; b) following 30 minutes of annealing at 300°C.

3. TMP 6, 13th Pass

Having seen the dramatic microstructure differences following the 12th passes of TMPs 6 and 7, an additional pass was conducted on a portion of the TMP 6 material. The higher strains in the late rolling passes apparently are significant in the resulting microstructure, primarily in the extent of recrystallization. A strain of 0.31 was achieved with the additional (13th) pass, and the accumulated strain increased from 2.5 to 2.9. Figure 14a represents the as-rolled condition for this pass 13 on TMP 6 material. Particles have further coarsened since the previous pass. Figure 14b shows the annealed condition for pass 13 of TMP 6 material. Recrystallization has occurred, along with further particle coarsening. Comparing the annealed microstructures of TMP 6 and TMP 7, pass 13 provides both larger recrystallized grains and particles. This can be attributed to a longer time at temperature.

4. TMP 8

Figure 15a represents the microstructure for the as-rolled condition. Comparing with the as-rolled condition for TMP 7, the TMP 8 precipitates are as homogeneously dispersed throughout the matrix, but have been elongated in the direction of rolling, the result of greater strain obtained at the last pass (0.44) compared to 0.34 of the TMP 7 process. Recovered areas are more extensive are in the TMP 8 than TMP 7. Figure 15b is the microstructure of the annealed condition for TMP 8. Particles have coarsened considerably with an additional 30 minute anneal. The microstructure appears to be fully recrystallized, whereas in

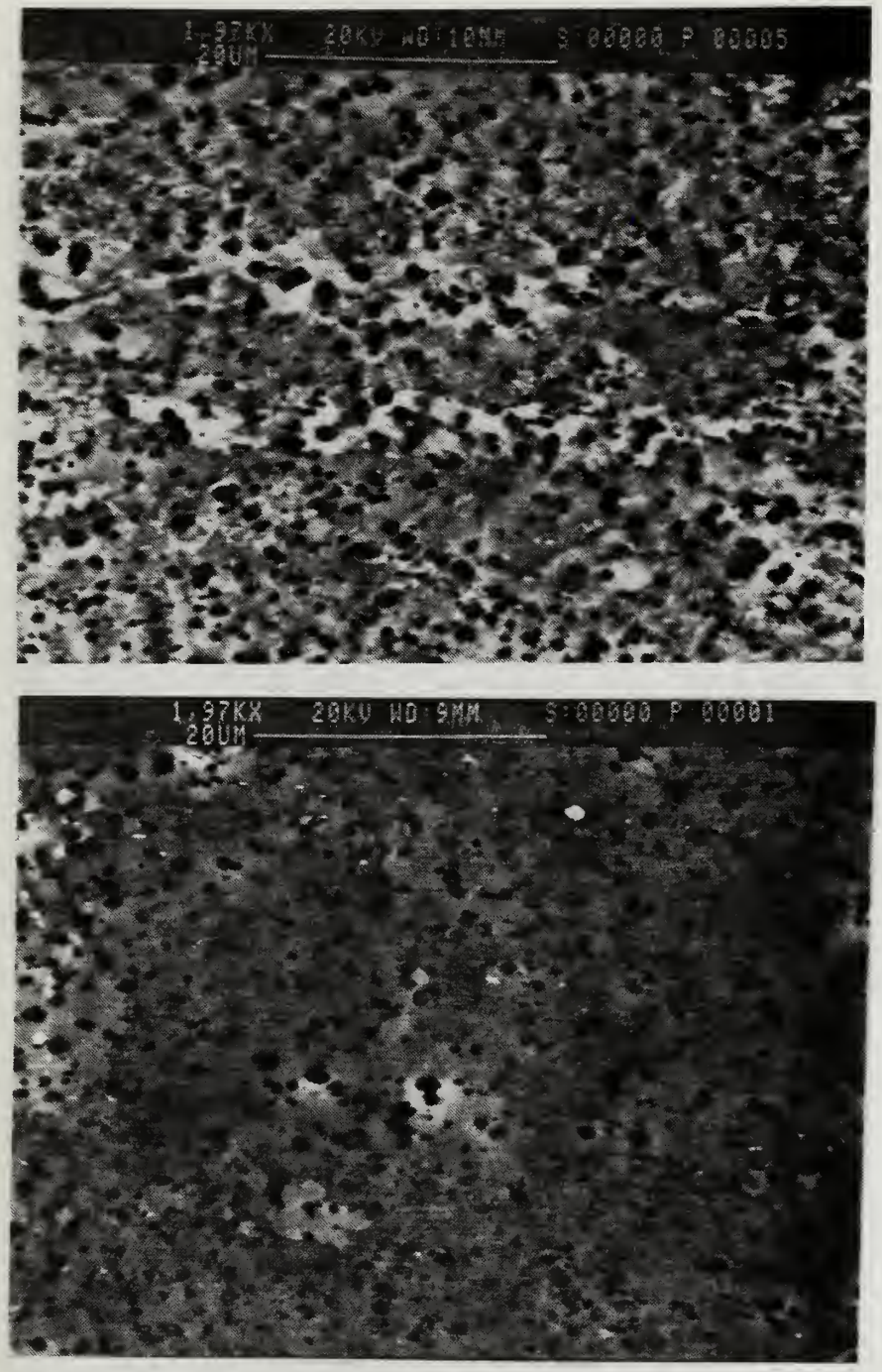

Figure 13. Backscattered SEM micrograph showing Al-10Mg-0.1Zr alloy following pass 12 of TMP 7: a) in the as-rolled condition; b) following 30 minutes of annealing at 300°C.

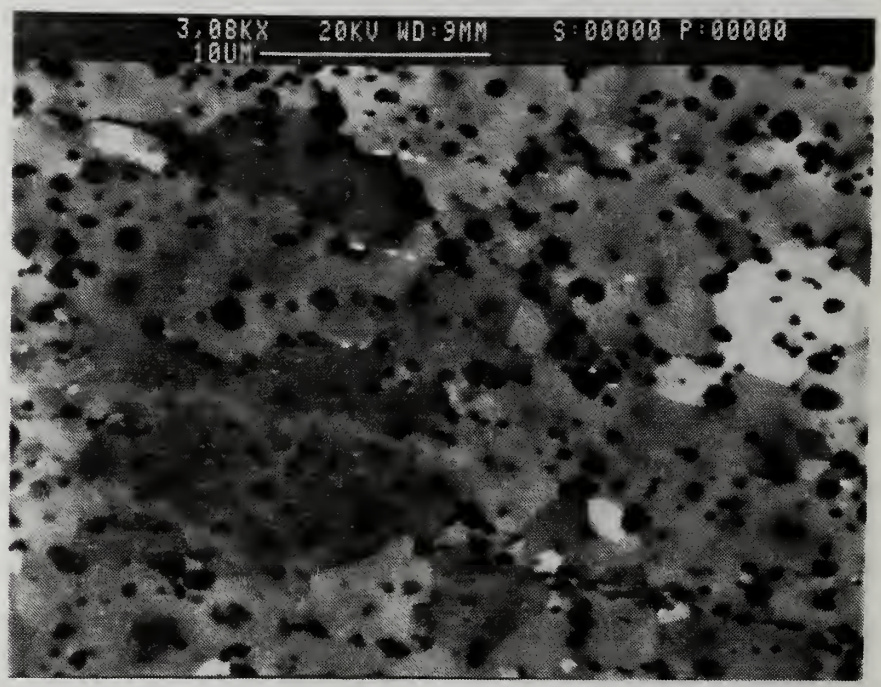

Figure 13. Backscattered SEM micrograph showing Al-10Mg-0.1Zr alloy following pass 12 of TMP 7: c) in the annealed condition at a higher magnification.

TMP 7 annealed condition some recovered areas were still present. Also, the particle size is noticeably larger than that of the TMP 7 material. Figure 15c represents the TMP 8 annealed condition at a higher magnification. Larger precipitates can be found within the new grain and along newly formed grain boundaries.

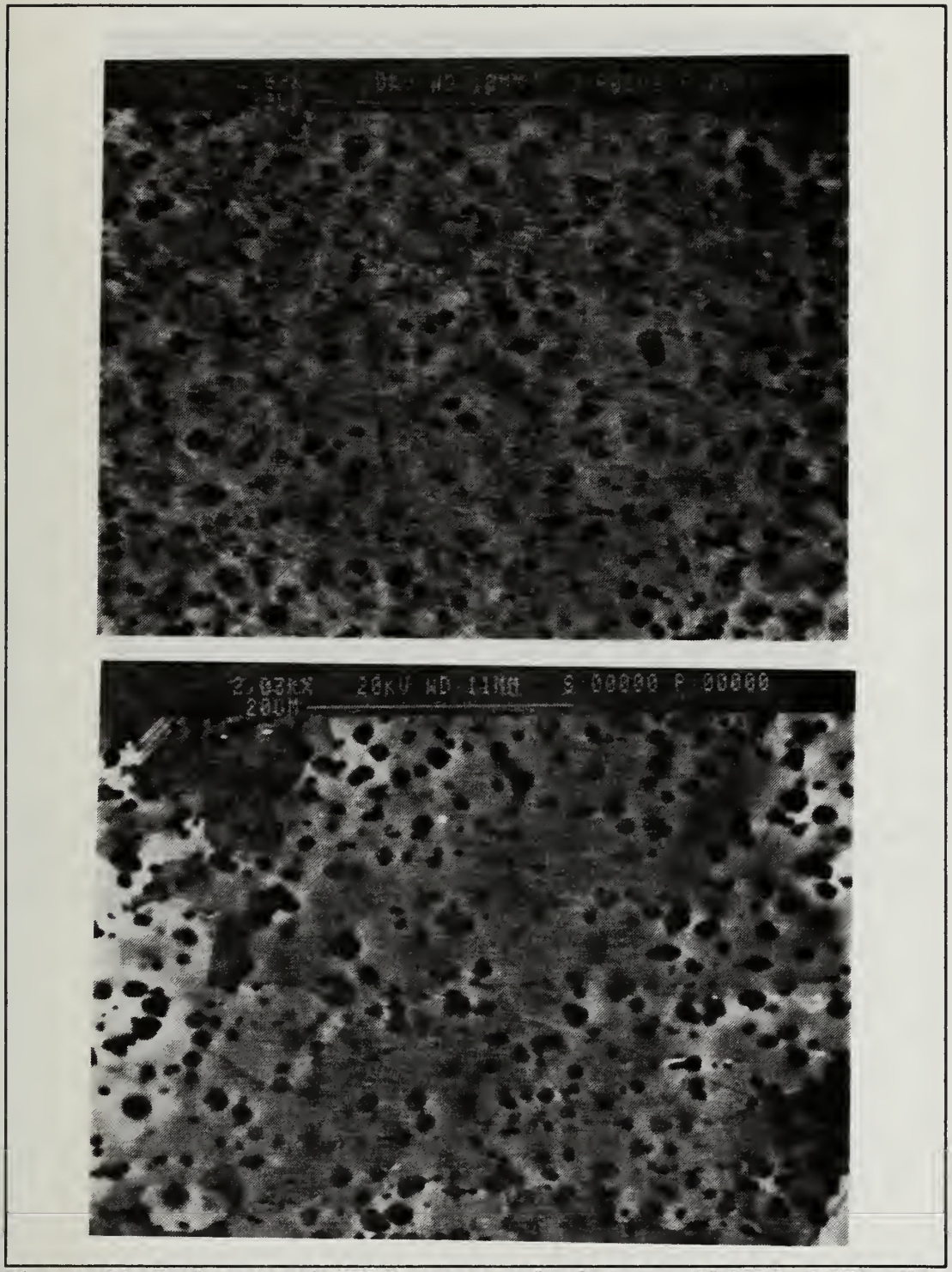

Figure 14. Backscattered SEM micrograph showing Al-10Mg-0.1Zr alloy following pass 13 of TMP 6: a) in the as-rolled condition; b) following 30 minutes of annealing at 300°C.

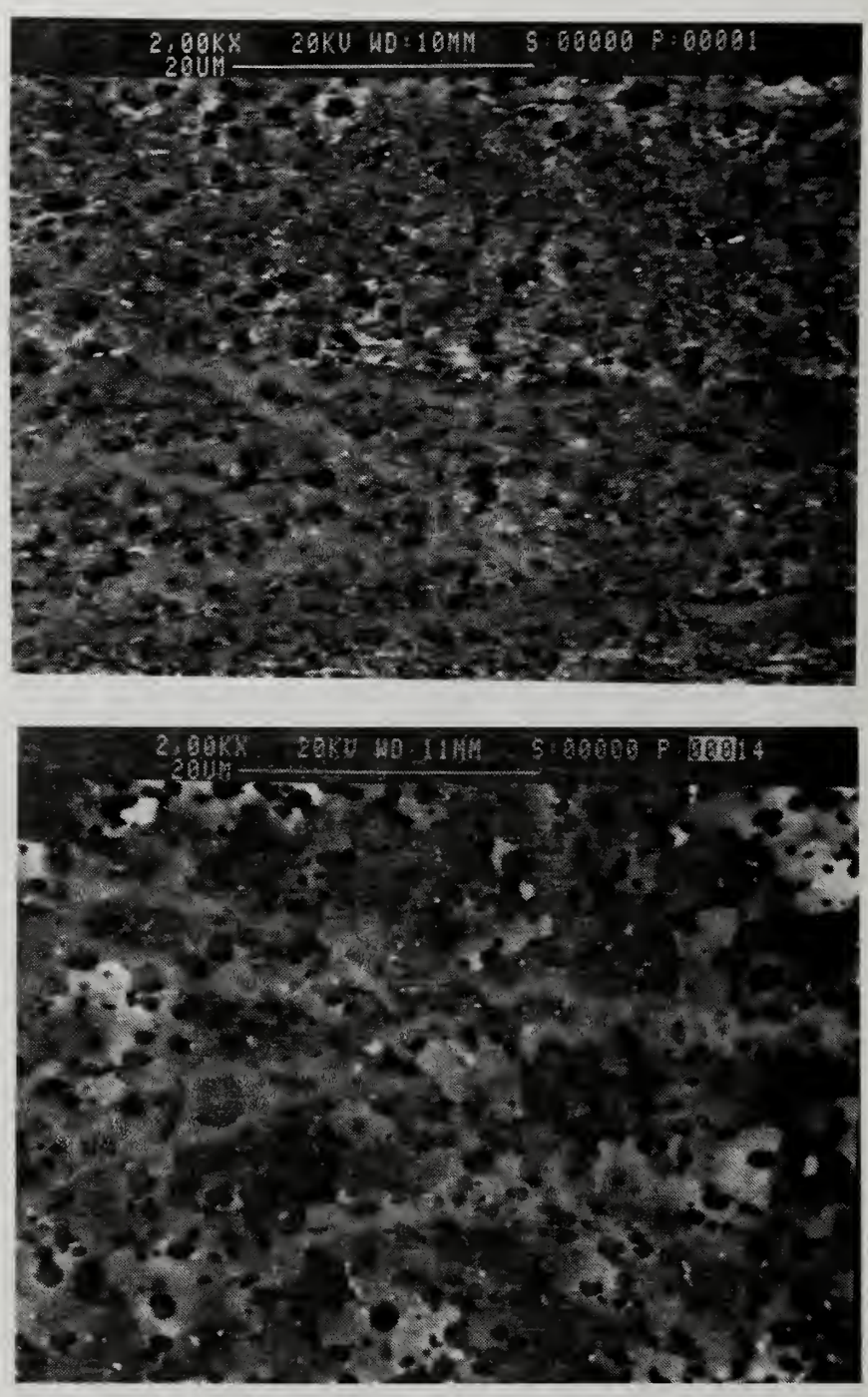

Figure 15. Backscattered SEM micrograph showing Al-10Mg-0.1Zr alloy following pass 10 of TMP 8: a) in the as-rolled condition; b) following 30 minutes of annealing at 300°C.

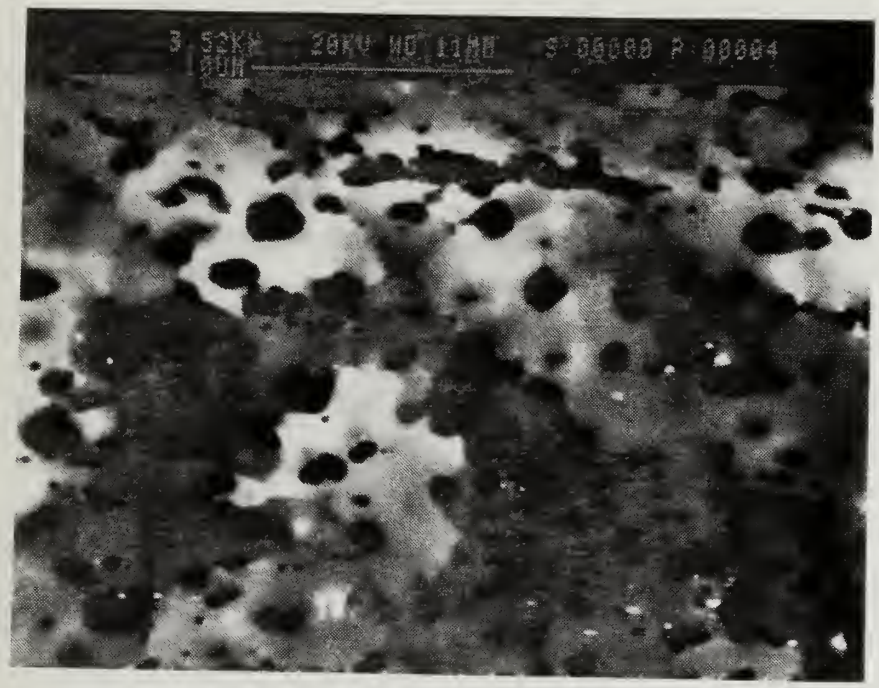

Figure 15. Backscattered SEM micrograph showing Al-10Mg-0.1Zr alloy following pass 10 of TMP 8: c) in the annealed condition at a higher magnification.

TABLE VIII. STRAIN RATE SENSITIVITY COEFFICIENTS

TRUE STRAIN	TMP 6	TMP 7	TMP 8
.1	.208	.485	.477

D. MECHANICAL TESTING RESULTS

As previously stated, the microstructure at the conclusion of a 30 minute anneal is similar to the microstructure prior to tensile testing. From the results of tensile testing, ductility, true stress-true strain and strain rate sensitivity characteristics were determined. All samples were tested 300°C at constant crosshead speeds of either 0.2 in/min (5.08 mm/min) or 0.02 in/min (.508 mm/min) and were pulled to failure.

1. Strain Rate Sensitivity Coefficient (m)

During tensile testing, values of crosshead position, strain, engineering stress and load were obtained. From these data, graphs of load versus crosshead position for each crosshead speed were plotted. After data reduction, values for true stress and true strain were calculated and plotted (Figures 22, 23, and 24). Following interpolation of true-stress values at a strain of 0.1 (10%) for tests at both strain rates, a graph of true stress versus strain rate on double log axes was plotted. Figures 16, 17, and 18 summarize these results. The slope of this graph ($m=\delta \ln\sigma/\delta \ln\dot{\varepsilon}$) is the approximate m value. The value of the strain rate sensitivity coefficient, m, is indicative of the material's resistance to localized necking. A strain of 0.1 was selected because the effect of the thermal gradient (see experimental procedure) was minimal at this early stage of the tensile testing. Table VIII summarizes the m values for each TMP.

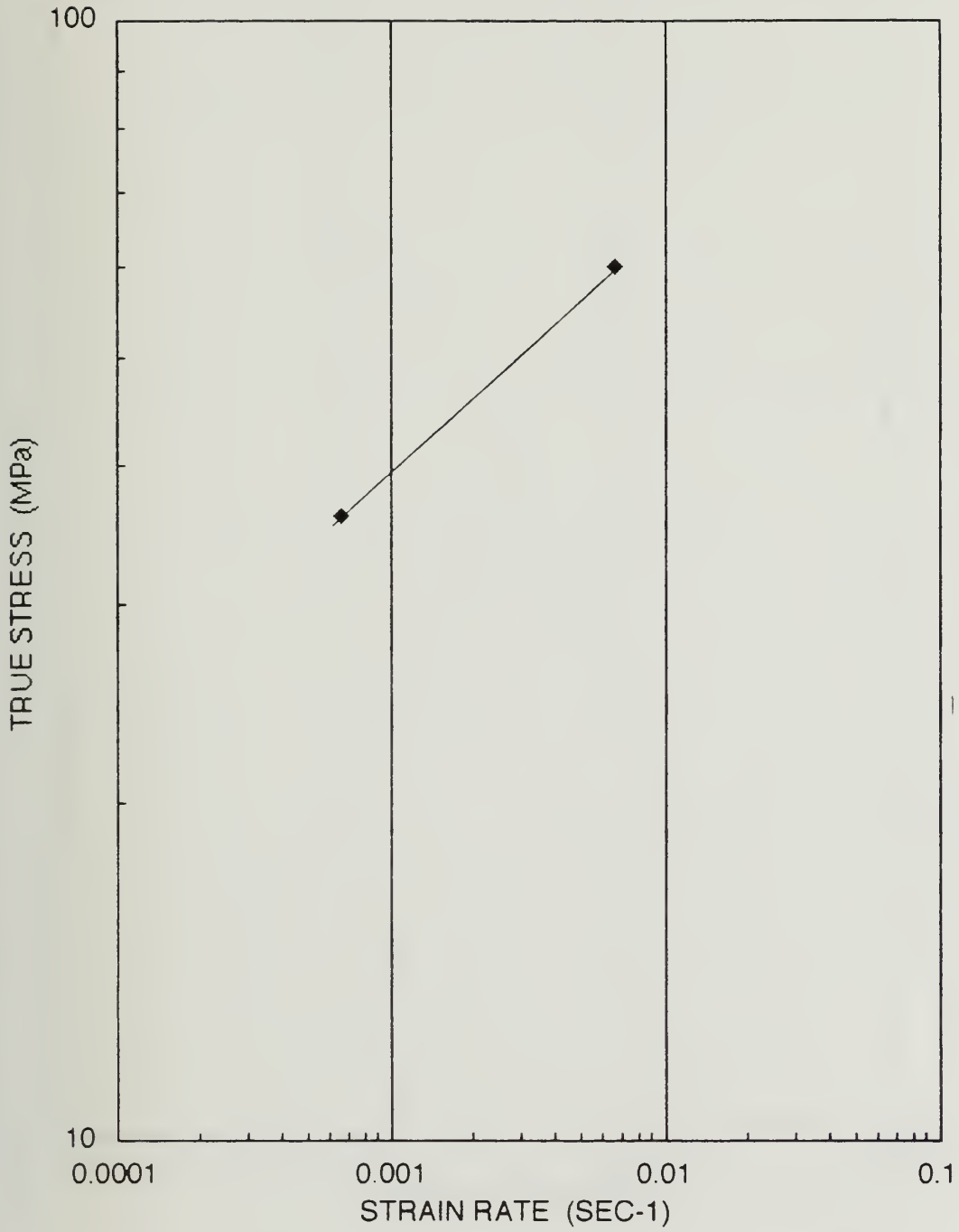

Figure 16. True Stress versus Strain Rate (m) for TMP 6.

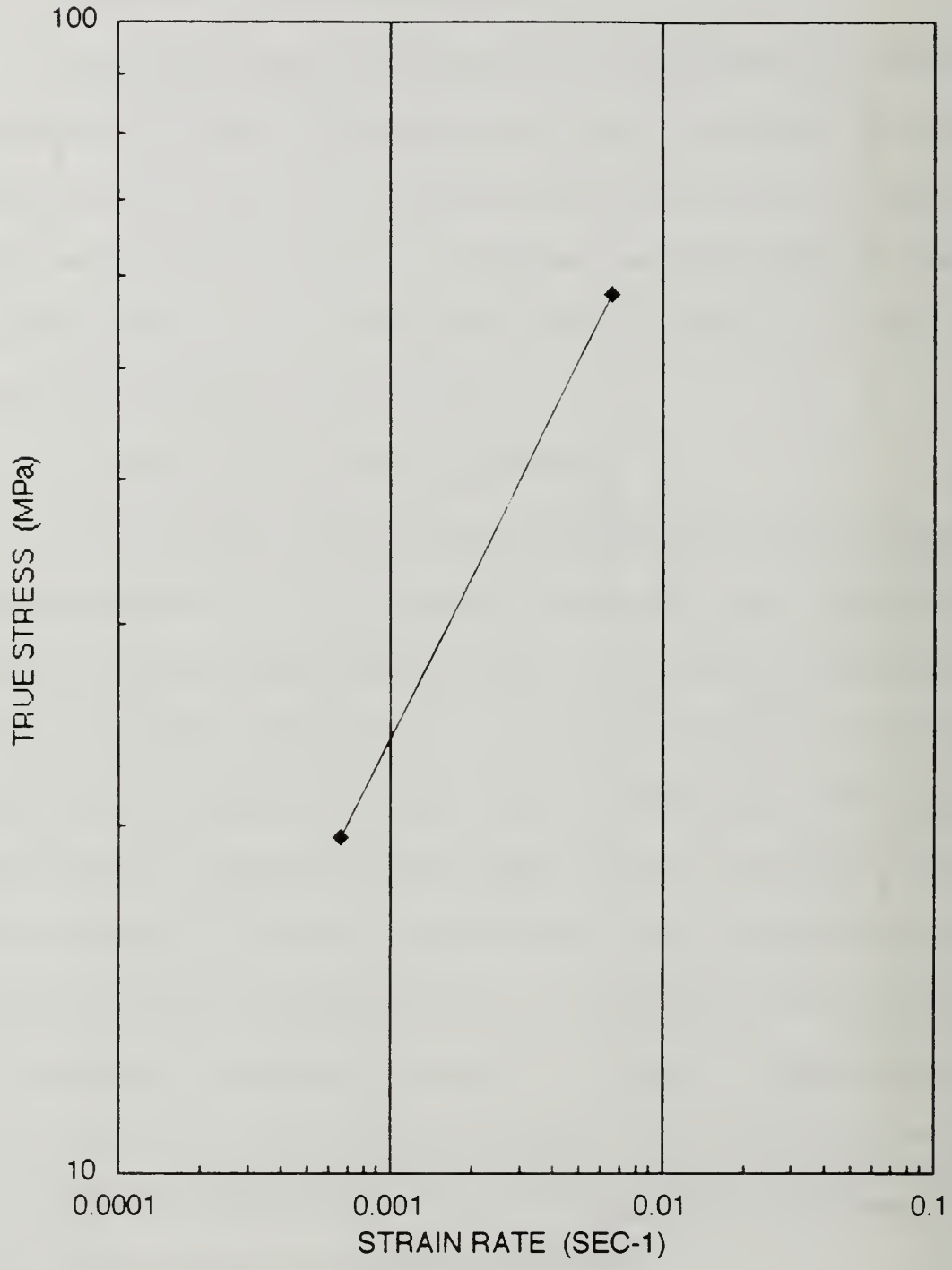

Figure 17. True Stress versus Strain Rate (m) for TMP 7.

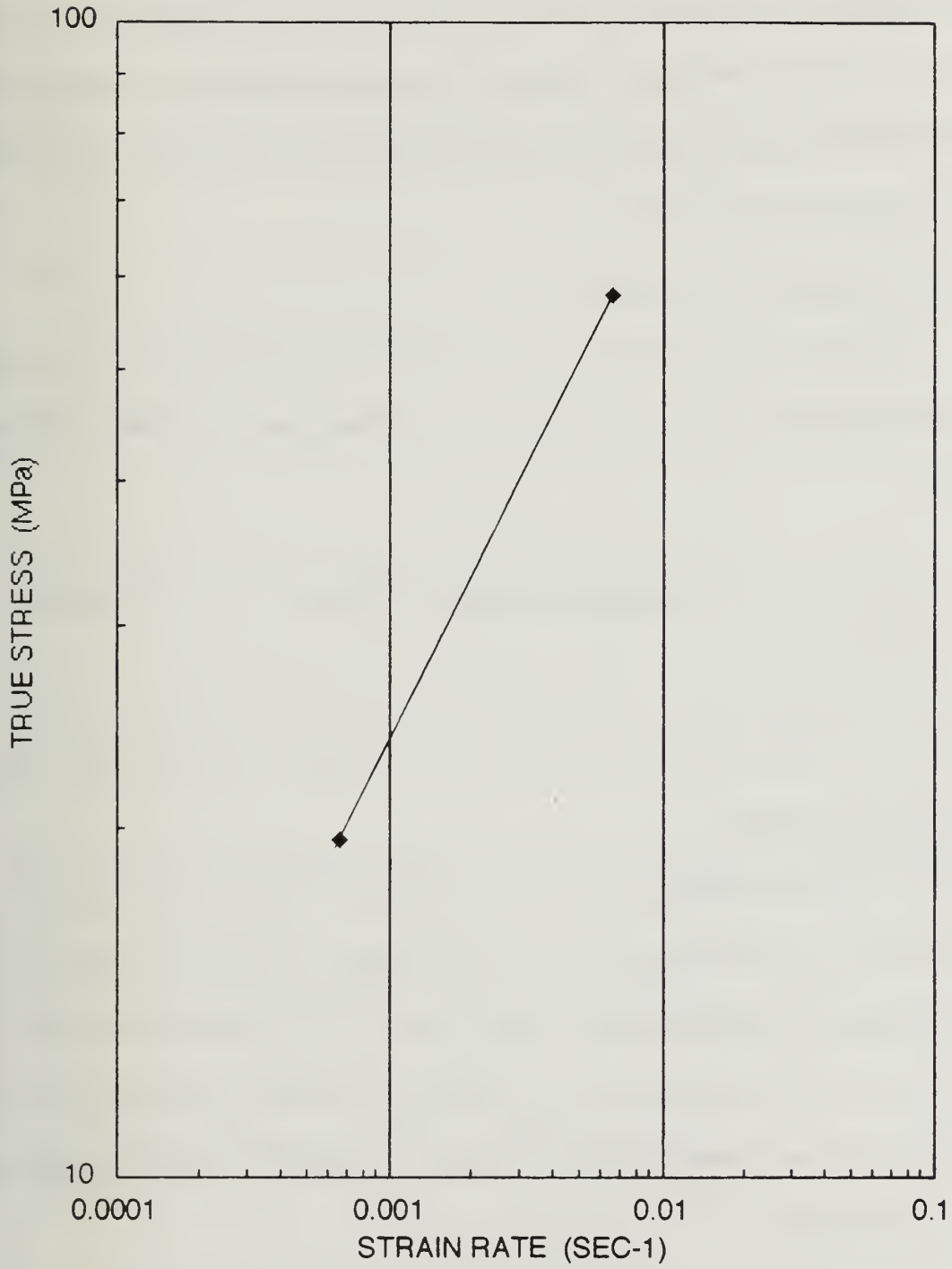

Figure 18. True Stress versus Strain Rate (m) for TMP 8.

Materials processed by TMPs 7 and 8 have very similar m values, while TMP 6 exhibits a significantly smaller one. Assessment of m at larger strains was not done due to the previously mentioned experimental problem. Nonetheless, strain rate sensitivity coefficients indicate that the TMP 7 and 8 are should behave more superplasticly than TMP 6.

2. Ductility Characteristics

Figures 19, 20, and 21 are graphs of ductility versus strain rate plotted on semi-logarithmic axes. Ductility was determined by the equation [Ref. 17].

$$\%\ Elongation(Ductility)=\frac{l_o-l_f}{l_o}\times 100 \qquad \textbf{Equation 9}$$

where l_o is the initial gauge length of 0.5 in (12.7 mm) and l_f is the final measured gauge length.

TMP 6 displayed minimal superplastic behavior, while TMP 7 and TMP 8 showed better superplastic responses. All failed samples exhibited the effect of the thermal gradient, for all specimens necked and may have prematurely failed at points where the temperature was at its greatest. Samples predominately failed at a point which was closer to the bottom grip, rather ideally failing at the middle of the gauge length.

In spite of these problems, ductility values reflect the extent of recrystallization and respective m values. TMP 7 and 8 both had ductility

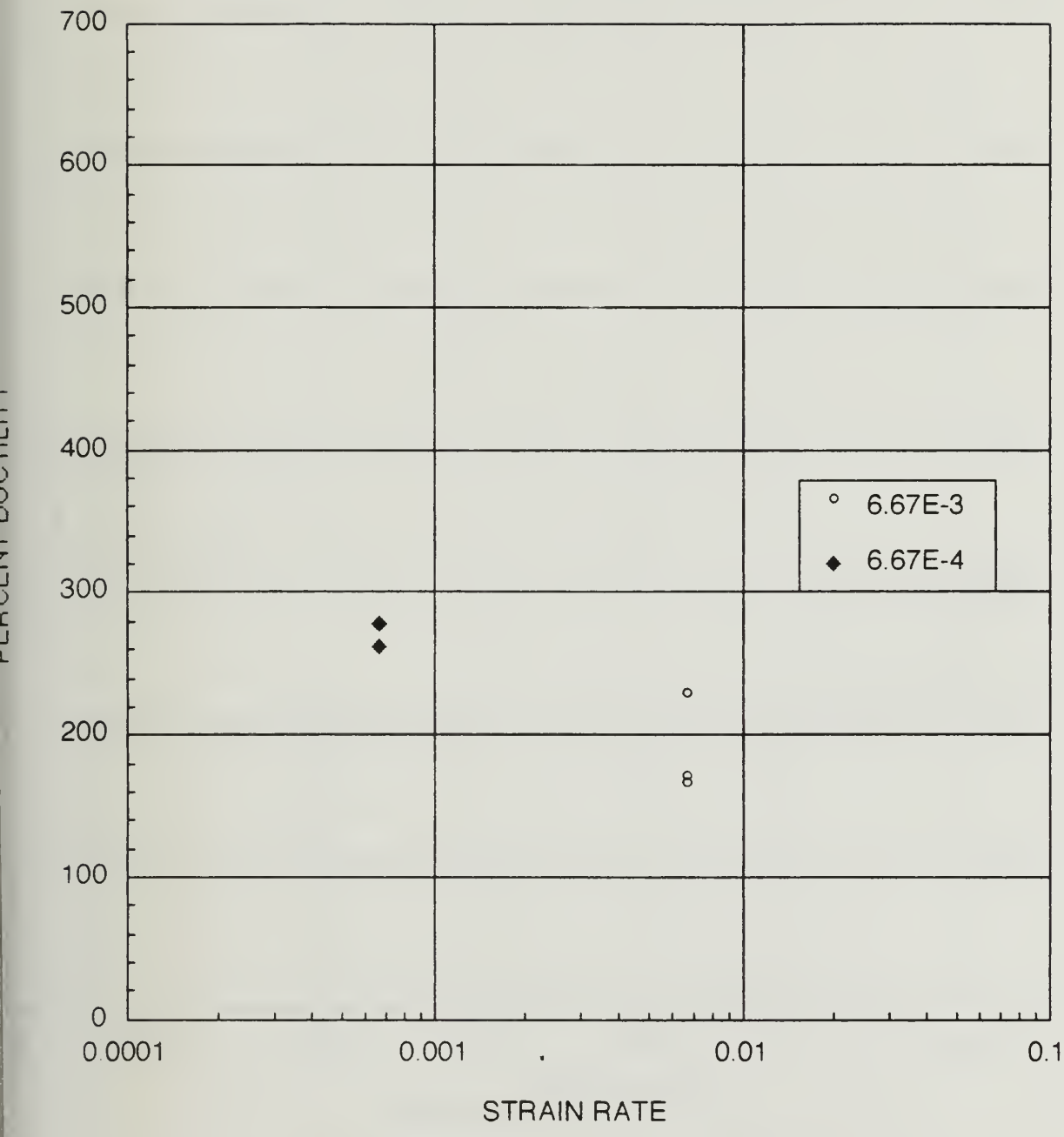

Figure 19. Ductility versus Strain Rate for TMP 6.

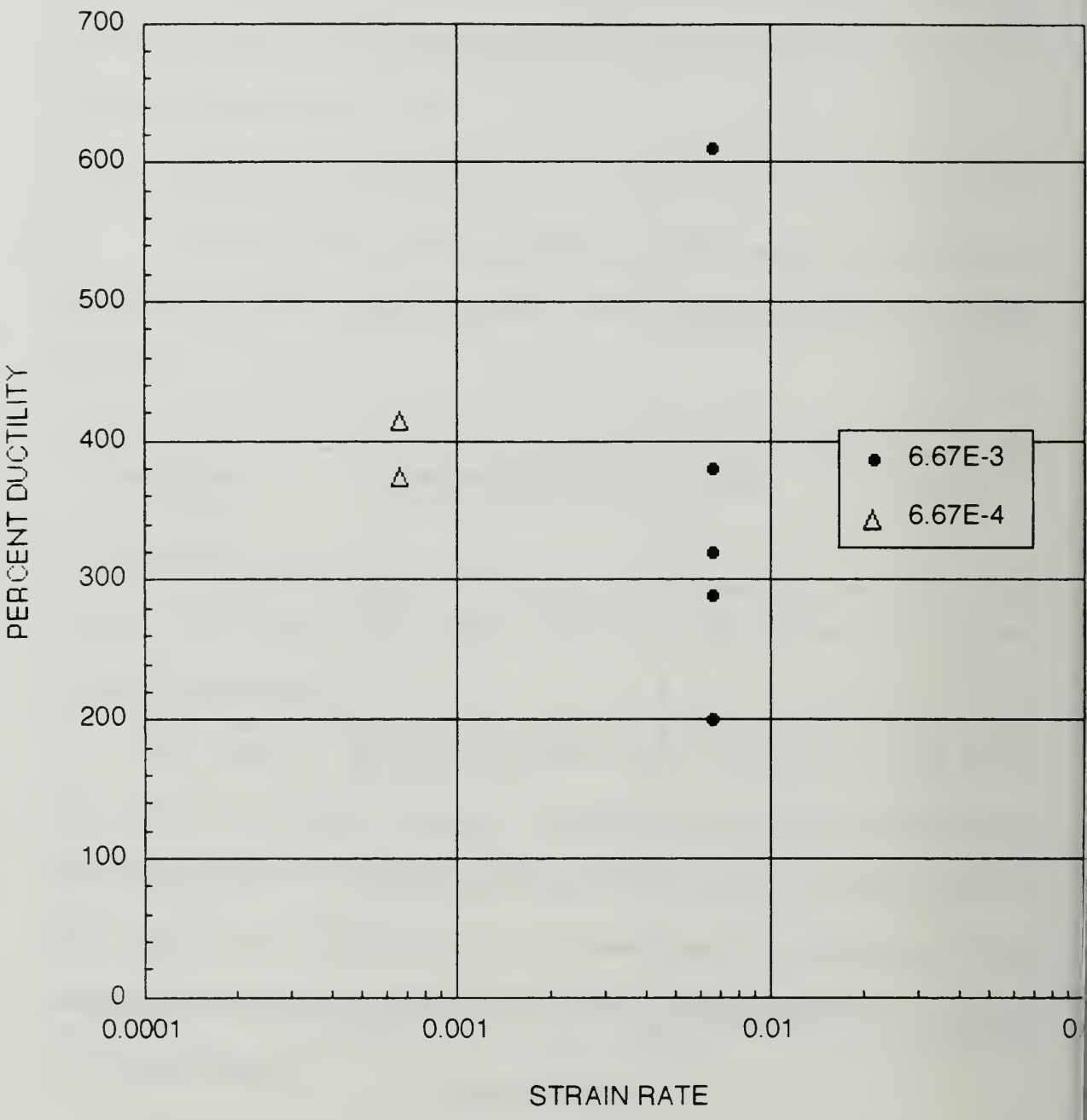

Figure 20. Ductility versus Strain Rate for TMP 7.

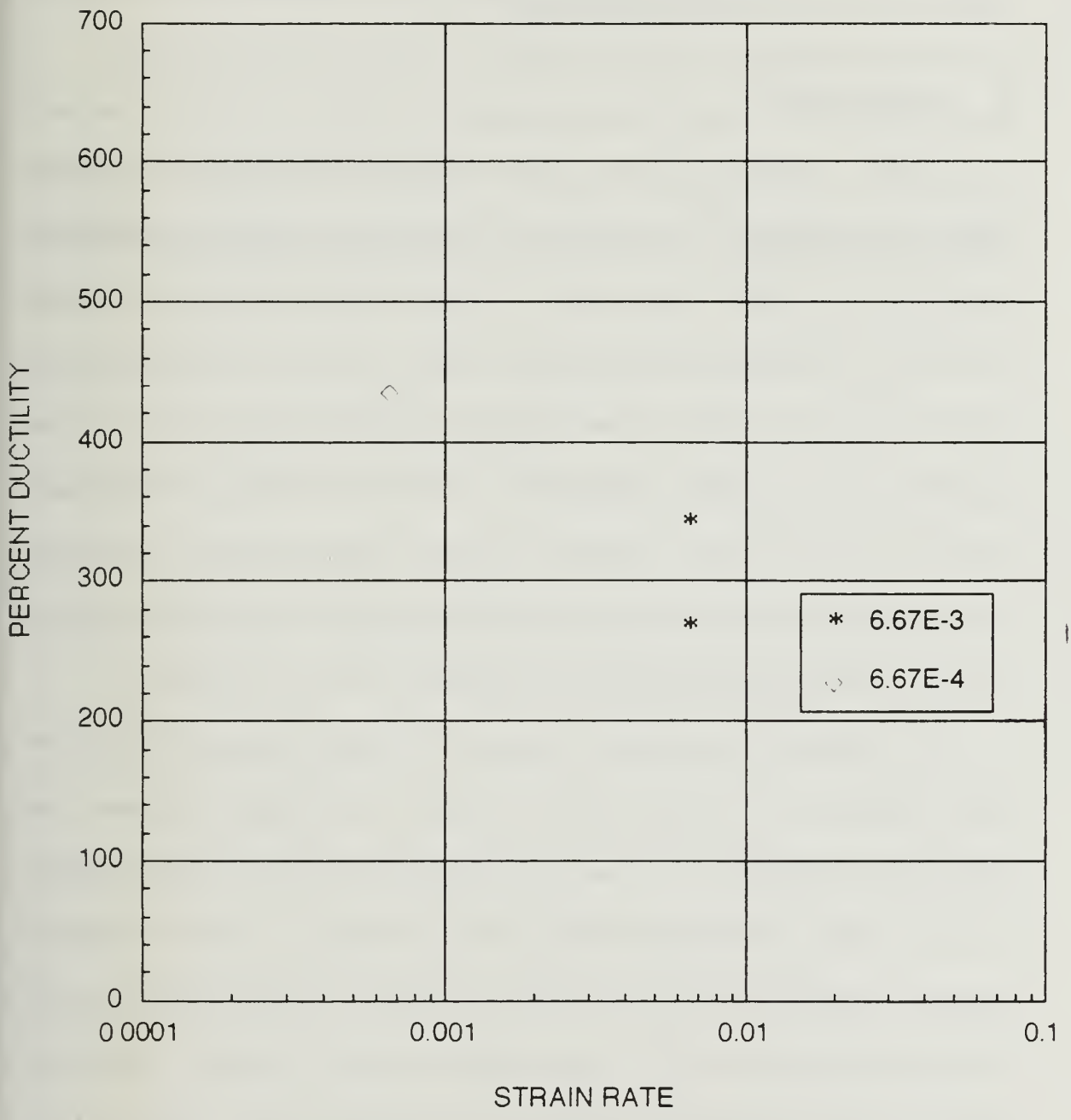

Figure 21. Ductility versus Strain Rate for TMP 8.

upwards of 400 percent, and perhaps exceeding 600 percent, whereas TMP 6 had ductility less than 300 percent. Overall, for each TMP higher ductilities were achieved at the lower strain rate (6.67E-4).

E. DISCUSSION

In the early stages of the TMP, dislocation generation and particle precipitation dominate. The β phase particles initially precipitate on prior grain boundaries, and further rolling helps homogenize the distribution of the beta precipitates. Deformation bands develop within the matrix, as well as highly strained areas surrounding larger, coarsened particles. These bands provided nucleation sites for further precipitation, and additional time at temperature allowed in recovered areas to develop. Thus the TMP produced an essentially unrecrystallized condition. At the onset of tensile deformation, which included a preheat interval, recrystallization and refinement of the grains resulted.

These results indicate that the thermomechanical process, particularly the strains obtained in the late passes of each TMP, directly influence the microstructural development. Larger strains attained in the later passes resulted in a more fully recrystallized structure that developed as a result of particle stimulated nucleation. The TMP 6 schedule developed by Gorsuch [Ref. 8] which had previously produced fine, recrystallized structure and high superplastic ductility did not accomplish this here. In this research, using TMP 6 did not produce particle sizes great enough to initiate particle stimulated nucleation, but

with an additional (13th) pass of a large strain, fine recrystallized structure resulted. This suggests that the onset of recrystallization is very sensitive to the interaction between strain and particle size for this alloy.

Mechanical testing results, although somewhat incomplete and inaccurate due to the thermal gradients experienced along the furnace length, indicate superplastic responses for material that was recrystallized. Such recrystallized material had higher values of strain rate sensitivity coefficient and ductility values.

V. CONCLUSIONS AND RECOMMENDATIONS

A. CONCLUSIONS

The conclusions and observations of this research are as follows:

1. Strains achieved in the later passes of TMP play a significant role in the superplastic response of a material. Ductilities and strain rate sensitivity coefficients significantly increased when larger strains were applied in the later passes of the TMP.

2. Comparable superplastic responses were obtained in a ten pass rolling schedule that incorporated a greater strain in the last pass.

3. Accumulated strain alone is not directly indicative of a material's hardness or superplastic potential.

4. Microstructural evidence demonstrated the development of an Al-10Mg-0.1Zr alloy that was thermomechanically processed. Precipitation on prior grain boundaries, deformation bands, particle coarsening, recovery and indications of particle stimulated nucleation of recrystallization were the observed sequence of the microstructural development.

5. Material that had higher reductions-greater strains during development had a more refined substructure, comprised of equiaxed recrystallized grains.

6. The effect of an additional pass of a higher strain was a more recrystallized microstructure compared with a recovered, less recrystallized microstructure.

B. RECOMMENDATIONS

The recommendations for further research are as follows:

1. Investigate the superplastic responses of TMP 7 and TMP 8 utilizing a separately controllable, multi-zone, furnace. Determine more substantial stress/strain relationships.

2. Conduct further tensile tests at varying strain rates in order to determine the strain rate influence upon the strain rate sensitivity coefficient (m).

3. Conduct quantitative microstructural analysis to determine volume fraction of precipitates, particle size and their influence upon the microstructural development, particularly particle stimulated nucleation of recrystallization.

4. Perform developed TMP schedules upon other aluminum alloys. Determine if higher strains achieved in later passes result in higher ductilities for other aluminum alloys.

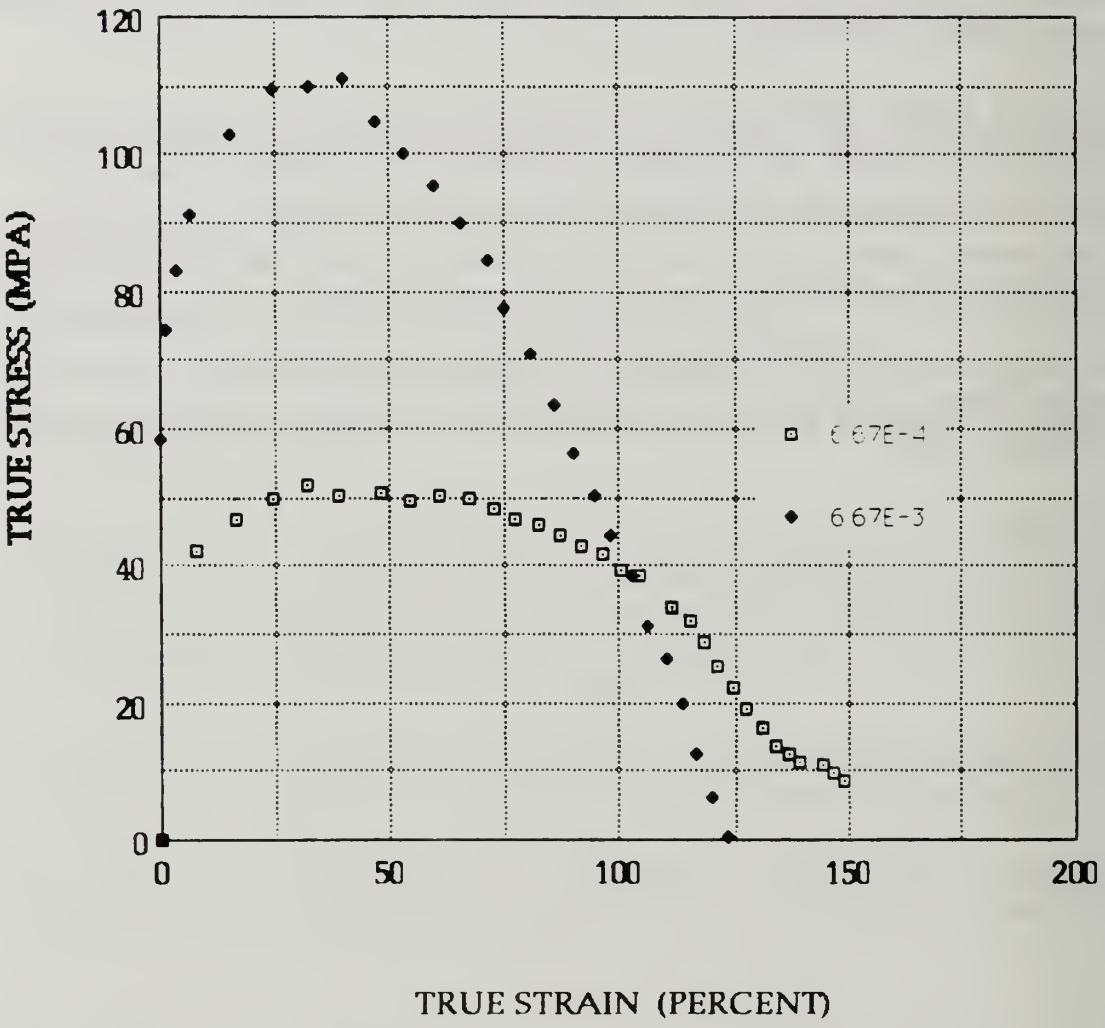

Figure 22. True Stress versus True Strain for TMP 6.

APPENDIX B

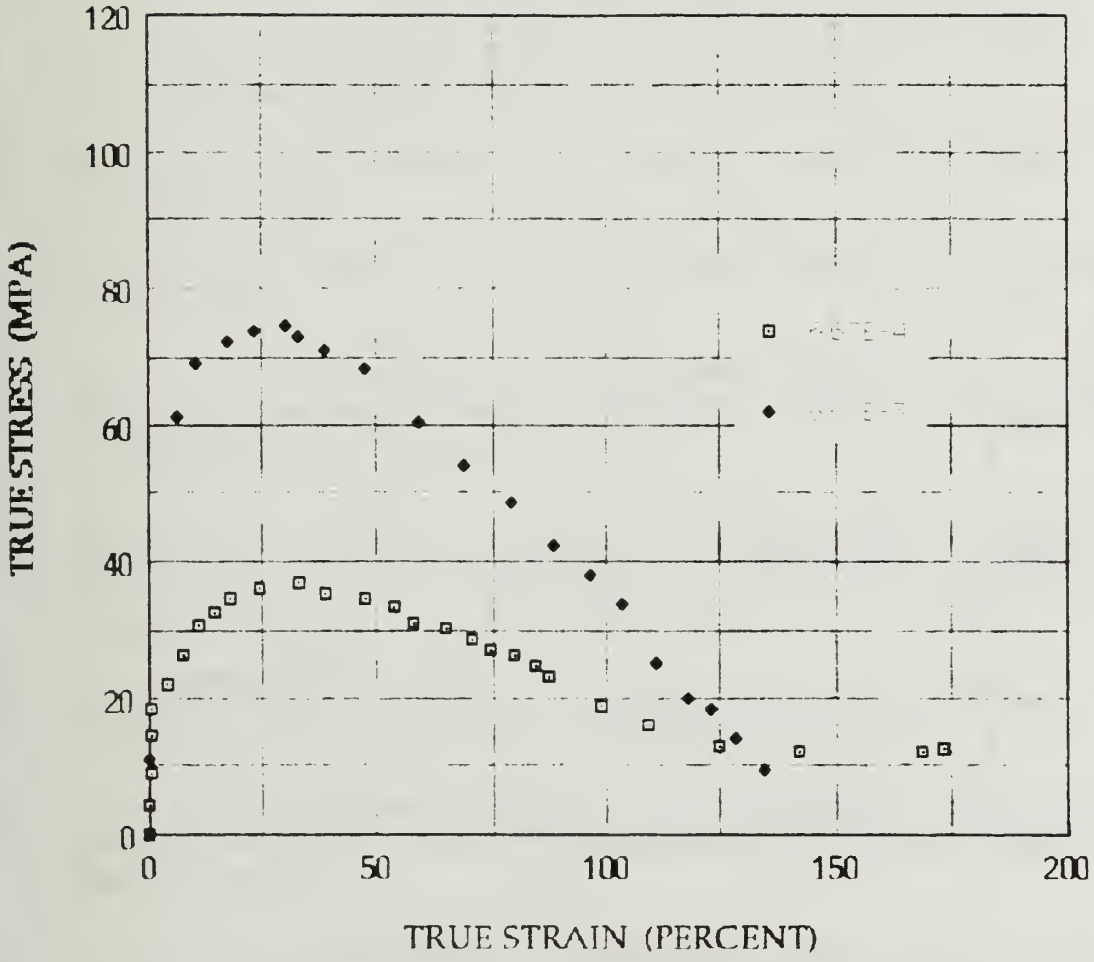

Figure 23. True Stress versus True Strain for TMP 7.

APPENDIX C

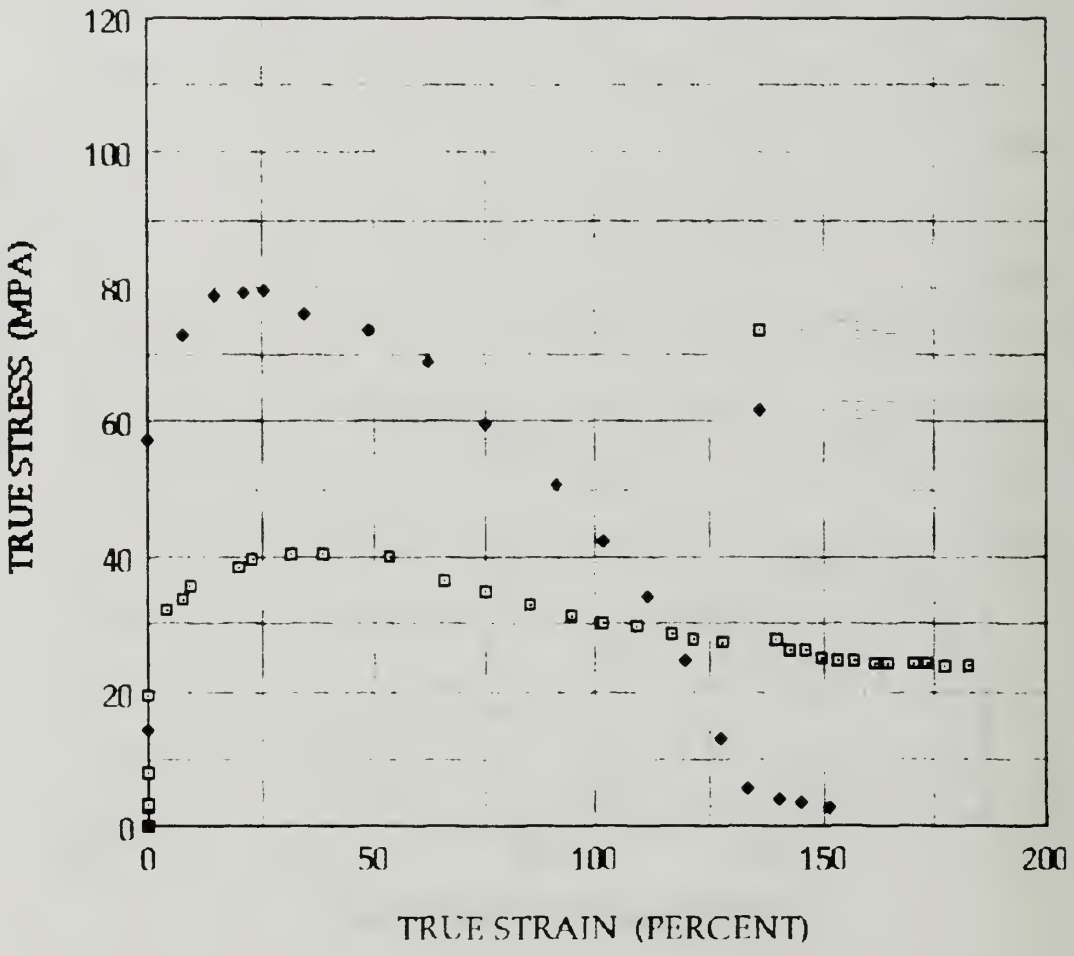

Figure 24. True Stress versus True Strain for TMP 8.

LIST OF REFERENCES

1. Baudelet, B., "Industrial Aspects of Superplasticity," *Material Science and Engineering*, A137, pp. 41-55, 1991.

2. "Aluminum Alloys--Contemporary Research and Applications," edited by Vasudevan, A.K., and Doherty, R.D., *Treatise on Materials Science and Technology*, Vol. 31, Academic Press Inc., 1989.

3. Anderson, R.J., *Metallurgical and Chemical Engineering*, No. 10, 523.

4. Watts, B.M., et. al., "Superplasticity in Al-Cu-Zr Alloys Part I: Material Preparation and Properties," *Metal Science*, June 1976.

5. *Metals Handbook*, Tenth Edition, Vol. 2, edited by Davis, J.R., et. al., ASM International, 1990.

6. Mondolfo, L.F., "Aluminum Alloys: Structure and Properties," Butterworths, London, 1976.

7. Sherby, O.D., and Wadsworth, J., "Development and Characterization of Fine-Grain Superplastic Materials," *Deformation, Processing, and Structure*, American Society for Metals, 1987.

8. Gorsuch, T.E., *The Roles of Strain and Reheating Interval in Continuous Recrystallization During the Thermomechanical Processing by Warm Rolling of an Al-Mg Alloy*, Master's Thesis, Naval Postgraduate School, Monterey, California, 1989.

9. "Superplasticity and Superplastic Forming," edited by Hamilton, C.H., and Paton, N.E., *The Minerals*, Metals & Materials Society, 1988.

10. Meyer, Chris D., *Processing, Microstructure and Superplasticity in Al-Mg-Mn Alloys*, Master's Thesis, Naval Postgraduate School, Monterey, California, December 1991.

11. Lee, E.W., and McNelley, T.R., "Microstructure Evolution During Processing and Superplastic Flow in a High Magnesium Al-Mg Alloy," *Materials Science and Engineering*, Vol. 93, 1987.

12. Humphreys, F.J., "Nucleation of Recrystallization in Metals and Alloys with Large Particles," Department of Metallurgy and Materials Science, Imperial College, London, SW7, England.

13. Pilling, J., and Ridley, N., *Superplasticity in Crystalline Solids,* The Institute of Metals, Book 441, 1989.

14. Hales, S.J., and McNelley, T.R., "Microstructural Evolution by Continuous Recrystallization in a Superplastic Al-Mg Alloy," *Acta Metall.,* Vol. 36, No. 5.

15. Alcoa Technical Center, Ltr., August 1984.

16. Crooks, R., Kalu, P.N., and McNelley, T.R., "Use of Backscattered Electron Imaging to Characterize Microstructures of a Superplastic Al-10Mg-0.1Zr Alloy," *Scripta Metallugrica et Materialia,* Vol. 25.

17. *Metals Handbook,* Ninth Edition, Vol. 8, Mechanical Testing, American Society for Metals, 1985.

INITIAL DISTRIBUTION LIST

		No. Copies
1.	Defense Technical Center Cameron Station Alexandria, Virginia 22304-6145	2
2.	Library, Code 052 Naval Postgraduate School Monterey, California 93943-5002	2
3.	Naval Engineering Curricular Office, Code 570 Naval Postgraduate School Monterey, California 93943	1
4.	Professor T. R. McNelley, Code ME/Mc Department of Mechanical Engineering Naval Postgraduate School Monterey, California 93943	4
5.	Adjunct Professor P. N. Kalu, Code ME/Mc Department of Mechanical Engineering Naval Postgraduate School Monterey, California 93943	1
6.	Adjunct Professor R. Crooks, Code ME/Mc Department of Mechanical Engineering Naval Postgraduate School Monterey, California 93943	1
7.	Dr. Lewis Sloter, Code AIR 931A Headquarters, Naval Air Systems Command Washington D.C. 20361	1
8.	LT Peter C. Lyle 110 Barbara St. Lowell, Massachusetts 01854	1

DUDLEY KNOX LIBRARY
NAVAL POSTGRADUATE SCHOOL
MONTEREY CA 93943-5101

DUDLEY KNOX LIBRARY
3 2768 00308035 9